2009

Atomistic simulations of lipid bilayers in the presence of dimethylsulfoxide

Raghava Alapati
Louisiana State University and Agricultural and Mechanical College

ATOMISTIC SIMULATIONS OF LIPID BILAYERS IN THE PRESENCE OF DIMETHYLSULFOXIDE

A Thesis

Submitted to the Graduate Faculty of the
Louisiana State University and
Agricultural and Mechanical College
in partial fulfillment of the
requirements for the degree of
Master of Science in Mechanical Engineering

in

The Department of Mechanical Engineering

By
Raghava Alapati
B.Tech. Jawaharlal Nehru Technological University, Hyderabad, India, 2006
December 2009

ACKNOWLEDGEMENTS

I would like to take this opportunity to express my sincere thanks to all the people who directly or indirectly have been instrumental to my success throughout my master's study here at Louisiana State University. First and foremost I would like to thank Dr. Ram Devireddy & Dr. Dorel Moldovan, my outstanding graduate advisors for having been so supportive, for inspiring me to stretch myself over my limits and for their never ending enthusiasm. I am extremely appreciative for their guidance both, from a technical and professional front. My next acknowledgements are due to my parents and family members back in India, who were always behind me with their prayers, love and blessings, encouraged me and provided tremendous support throughout my life. Without their help, I wouldn't have been here.

Last but not the least, I would like to thank all my colleagues in the Bioengineering and Materials Simulations Laboratory and all my friends whose support was very valuable during my Master's study at LSU.

TABLE OF CONTENTS

LIST OF TABLES

LIST OF FIGURES

NOMENCULATURE

J	flux
U_s	Solute mobility
c_s	Solute concentration
L_{ss}	Generalized conductance between non-electrolyte - non-electrolyte
L_{sw}	Generalized conductance between non-electrolyte - solvent
$\Delta\mu_s$ and $\Delta\mu_w$	Chemical potential differences
$\frac{d\mu_s}{dx}$	Chemical potential gradient
c_s^I and c_s^{II}	Concentrations of the two non-electrolyte solutions
Δc_s	Concentration difference
R	Universal gas constant
ΔP	Change in pressure
$\overline{V}$	Partial molar volume
T	Temperature
J_v	Volume flux
J_D	Exchange flux
L_p	Hydraulic conductivity
σ	Reflection coefficient
ω	Solute permeability
F_i	Momentary force on each atom
m	Mass
r_i	Position of particle *i*

t	Time
V	Negative gradient of the potential energy function
$V_{bond-strech}$	Harmonic potential representing the interaction between atomic pairs where atoms are separated by one covalent bond
K_{ij}	Force constant
r_{ij}^{0}	Equilibrium length of the bond
θ_{ijk}^{0}	Bond angle
$V_{bond-angle}$	Potential associated with the alteration of bond angle
$V_{rotate-along-bond}$	Torsion angle potential
K_{ijkl}	Force constant
q_i and q_j	Charges
ε_o	Permittivity of free space
ε_r	Relative permittivity
r_{ij}	Distance between the atoms
r	Position
v	Velocity (the first derivative of position with respect to time)
a	Acceleration (the second derivative of position with respect to time)
b	Jerk (the third derivative of position with time).
g(r)	Radial distribution function
N(r)	Number of atoms in spherical shell at distance r and thickness dr from a reference atom
P	Number density
θ_α	Angle between the molecular α-axis and the bilayer normal (z-axis)

$S_{\alpha\beta}$	Order parameter tensor
S_{CD}	Deuterium order parameter

ABSTRACT

In a typical cryopreservation protocol, the system to be preserved is first equilibrated with chemicals known as cryoprotective agents (CPAs). CPAs have been shown to alleviate cell damage from either the solute effects or the formation of intracellular ice during the subsequent freezing process. Thus, an extensive body of literature reporting the effects of CPAs on cellular systems has been accumulated over the last 50 years; detailing largely experimental interactions between cell systems and chemicals. Recent advances in computational methodology now offer an additional dimension in our ability to understand the molecular interactions between cell membranes, idealized as lipid bilayers and CPAs at atomistic scales. Computer simulations provide unique capabilities for analyzing biomembrane properties from atomistic perspective with a degree of detail that is hard to reach by other techniques. Molecular Dynamic (MD) simulations have been performed on phospholipid bilayers composed of Dimyristoylphosphatidylcholine (DMPC) lipids. The focus of our MD simulations was on the development of a fundamental understanding of the effects of low and moderate concentrations of dimethylsulfoxide (DMSO) on lipid bilayers membranes when exposed symmetrically or asymetrically to the water-DMSO solution. The molecular dynamic investigations show that the increase in concentration of DMSO leads to increase in area per lipid which in turn decreases the thickness of the bilayer. Moreover, the DMSO also has a significant effect on several other structural properties such as ordering of lipid tails and dipolar orientation ordering of the water molecules located near the water-bilayer interface.

1 INTRODUCTION

1.1 Cryobiology

Cryobiology is the branch of science that studies the effects of low temperatures on biological material. Cryobiology as an applied science is primarily concerned with low temperature preservation, commonly denoted as cryopreservation. Cryopreservation refers to a technique of storing living organisms at extremely low temperatures such as -196 $^{\circ}$C [1], in suspended animation for extended periods of time. Cryopreservation techniques are developed for the preservation of various biological systems such as, microorganisms, isolated tissue cells, small multi-cellular organisms and even more complex organisms such as embryos. These techniques have been successfully applied to a variety of mammalian systems such as red blood cells, lymphocytes, platelets, granulocytes, gametes and embryos, hepatocytes, bone marrow stem cells, cornea and skin, pancreatic tissue, heart and kidney, etc. as reviewed by Mazur [1] and McGrath [2]. Cryopreservation of cells is guided by the "Two-Factor Hypothesis" of American cryobiologist Peter Mazur [1], which states that rapid cooling kills cells by intracellular ice formation (IIF) and excessively slow cooling kills cells by either electrolyte toxicity or mechanical crushing [1]. During slow cooling ice forms extracellularly, causing water to osmotically leave cells, thereby dehydrates them. Due to dehydration and phase transition of water to ice, cells suffer severe osmotic stress and ice crystal damage during freezing and thawing. One of the most effective known ways to minimize the effect due to dehydration and IIF is to add chemical compounds to the culture prior to its freezing. These chemical compounds are usually referred to as cryoprotective agents (CPAs) and are used in cryopreservation for protecting cells and organs from freezing injuries while freezing. Advantage of CPA was first found in 1948 [3] in which they showed that cells can be protected from freeze damage by the

addition of glycerol. Subsequent studies have shown that compounds such as ethylene glycol [4], dimethylsulfoxide [5], polyethylene glycol [6], polyvinyl pyridine and others have the ability to protect cells from freeze damage. Cryoprotective solutions act primarily by reducing the amount of ice that is formed at any given subzero temperature. If sufficient cryoprotectant could be introduced, freezing would be avoided and a glassy or vitreous state could be produced due to increase in viscosity [7]. In cryopreservation, the solute must penetrate the cell membrane in order to achieve increased viscosity inside the cell, so higher concentrations of cryoprotectants cannot be used, since they may cause osmotic and toxic damages [7].

To optimize the cryopreservation processes the transport of cryoprotectants across the cell membranes must be well understood. This transport can either be passive transport (transports through lipids) or active transport (transport through channels). Passive transport of water and cryoprotective solutes across the membranes of individual cells plays an important role in freezing of cells (cryopreservation), since low temperatures tend to diminish the relative importance of active transport processes [8]. Due to severity of external disturbances in passive transport process there are many complexities involved, because of which it is of great interest to obtain a proper understanding of transport phenomenon (passive transport) [9]. For uncoupled flow of a single species across a membrane it is often appropriate to model the transport according to Fick's law [10]. But, most cells cannot be preserved by freezing without the addition of some type of cryoprotective chemicals. These protective chemicals penetrate the cell, but the permeability of these compounds is not nearly as high as the permeability of the membrane to water. Any change in the concentration of solute (the cryoprotectant) or the solvent (water) will induce a flow of the other across the membrane. The complex transportation

phenomenon of water across such coupled processes are well characterized by irreversible thermodynamic Kedem-Katchalsky (K-K) [11-13] macroscopic models. It is a well defined model for coupled water and CPA transport.

1.2 Membrane Kedem-Katchalsky (K-K) Permeation Model

The free diffusion of a single non-electrolyte when the only driving force for solute flux is the chemical potential gradient of the solute is given by [14]

$$J_s = U_s c_s \left(-\frac{d\mu_s}{dx}\right) \tag{1.1}$$

Where J stands for the flux, U_s stands for the solute mobility, c_s stands for the solute concentration and $\frac{d\mu_s}{dx}$ stands for the chemical potential gradient.

Similarly, the coupled fluxes of a non-electrolyte and solvent (subscript "w") across a semi-permeable membrane, where the concentrations and hydrostatic pressures are unequal, are as follows:

$$J_s = L_{ss}\Delta\mu_s + L_{sw}\Delta\mu_w \tag{1.2}$$

$$J_w = L_{ws}\Delta\mu_s + L_{ww}\Delta\mu_w \tag{1.3}$$

Where J_s and J_w stand for the chemical potential of non-electrolyte and the solvent respectively, L_{ss} and L_{sw} stand for the generalized conductance between non-electrolyte - non-electrolyte and between non-electrolyte - solvent respectively, L_{ws} and L_{ww} stand for the conductance between solvent - non-electrolyte and solvent - solvent respectively. By Onsager reciprocal relation $L_{ws} = L_{sw}$ [13, 14].

The difference in chemical potentials in Eq. (1.2) and Eq. (1.3) are just inside each face of the membrane. Chemical potential is a continuous function of position across the membrane-

solution interface; if it were discontinuous, then infinite gradients would exist, a condition inconsistent with the presence of a finite flux. When the solutions are assumed to be well-stirred, the chemical potentials can be written in terms of the bulk concentrations of the solutions. From a practical point of view Eq. (1.2) and Eq. (1.3) can be made easier to use by rewriting the chemical potential differences $\Delta\mu_s$ and $\Delta\mu_w$ in terms of measurable concentrations c_s and pressures in the two solutions, as follows,

$$\Delta\mu_s = \overline{V}_s \Delta P + RT\Delta \ln c_s \tag{1.4}$$

$$\Delta\mu_w = \overline{V}_w \Delta P - \overline{V}_w RT\Delta c_s \tag{1.5}$$

Where Δc_s is the concentration difference between c_s^I and c_s^{II} , the concentrations of the two non-electrolyte solutions, ΔP stands for the change in pressure, $\overline{V}_s$ & $\overline{V}_w$ stand for the partial molar volumes of the two non-electrolyte solutions, *R* stands for the universal gas constant and *T* stands for the temperature.

Here the solution is assumed to be ideal and dilute; the effects of non-ideality and non-diluteness will be dealt later. It is assumed that there are no temperature gradients across the membrane. Another assumption that will prove very useful is that the concentration difference across the membrane is small relative to the average concentration in the bathing solutions. When this is the case, the logarithmic concentration difference that appears in Eq. (1.4) can be approximated as follows,

$$\Delta \ln c_s = \frac{\Delta c_s}{\overline{c_s}} \tag{1.6}$$

Where $\overline{c_s} = {(c_s^I + c_s^{II})}/{2}$. The error of approximation is a function of the concentration ratio

$r = {c_s^I}/{c_s^{II}}$. The error of approximation does not reach 10% until r =3.Now that the chemical potential differences can both be written in terms of pressures and concentrations, Eqs. (1.2) & (1.3) can be rewritten accordingly. But because ΔP and Δc_s can be expressed more conveniently by finding new set of fluxes whose conjugate driving forces are more simply related to the pressure and concentration differences. The new set of fluxes is,

$$J_v = L_{vv}\Delta P + L_{vD}\Delta\pi \tag{1.7}$$

$$J_D = L_{vD}\Delta P + L_{DD}\Delta\pi \tag{1.8}$$

Where J_v & J_D stand for volume flux and exchange flux respectively. The volume flux is a conjugate to ΔP and exchange flux is a conjugate to $RT\Delta c_s$. The other parameters present in Eqs. (1.7) & (1.8) can be expressed in terms of phenomological coefficients as follows,

Hydraulic conductivity or Flow conductivity,

$$L_P = \left(\frac{J_v}{\Delta P}\right)_{\Delta\pi=0} = L_{vv} \tag{1.9}$$

Reflection coefficient,

$$\sigma = -\frac{L_{vD}}{L_{vv}} \tag{1.10}$$

Solute permeability,

$$\omega = \left(\frac{J_s}{\Delta\pi}\right)_{J_v=0} \tag{1.11}$$

Aforementioned transport coefficients characterize the passive flux of a given solute and a given solvent through a given membrane. The physical significance of two of the coefficients is rather

clear; the hydraulic conductivity measures the volume flow induced by a hydrostatic pressure difference, and solute permeability measures the solute flux induced by a concentration difference, like the permeability. The meaning of reflection is less obvious but generally it measures the effectiveness induced by osmotic pressure difference and it also influences the rate of convection of solute by the volume flux. By the application of all these equations Kedem-Katchalsky equations had been formulated as,

$$J_v = L_p \Delta P - \sigma L_p \Delta \pi \tag{1.12}$$

$$J_s = \overline{c_s} J_v (1 - \sigma) + \omega \Delta \pi \tag{1.13}$$

Each term in the Kedem-Katchalsky equations can be associated with a specific physical process; this is intuitively satisfying. The first term in the volume flow equation can be regarded as the hydraulic flow induced by the hydrostatic pressure difference, and the second term, called osmotic flow or osmosis, is the contribution to the volume flux resulting from the osmotic pressure difference across the semi-permeable membrane. Similarly, the first term in the solute flux equation can be regarded as the rate at which solute is carried across the membrane (i.e convected) by the volume flux (this is often termed “solvent drag”), while the second term has the form of a diffusional component driven by the solute concentration difference. However satisfying this decomposition of the Kedem-Katchalsky equations may be, it must be remembered that each molecule of solvent and solute is acted upon by all driving forces, so the processes described above are not separable.

The Kedem-Katchalsky formalism explains the transportation phenomenon at macroscopic scale by phenomological laws; it does not really provide us a precise microscopic understanding of the phenomenon. To effectively optimize this transportation phenomenon it is very important

for us to obtain a better understanding at the microscopic scale. To understand the interactions of cells with water and CPA molecules, we first have to understand the interactions with cell membranes – or lipid bilayers as model systems. So the understanding of cell membranes is of tremendous biological importance.

1.3 Cell Membrane

The cell membrane separates the interior of the cell from the outside environment [15]. Cell membrane is the first part of cell which comes in contact with any nutrients, pathogen, or other molecules present in cellular environment. So understanding the cell membrane is of tremendous biological importance. Biological membranes are uniquely capable of a variety of functions due to the intrinsic properties of the membrane structure. For example, membranes are generally semi-permeable [16]. That is, most molecules cannot penetrate inside the membrane unless proteins facilitate their movement. This property allows the membranes of a cell to control the passage of materials moving across the cell membrane. Biological membranes contains a wide variety of molecules, primarily lipids and proteins; other constituents include: water, cholesterol, sugar groups, metal ions and carbohydrates [17] (see Fig 1.1). Cholesterol is not found in all types of membranes.

The lipid molecules in cell membrane are spontaneously arrange themselves so that non-polar, hydrophobic fatty acid tail regions are shielded from the surrounding polar fluid, causing the hydrophilic head region to associate with the cytosolic and extracellular faces of the resulting bilayer. The proteins usually span from one side of the phospholipids bilayer to the other (integral proteins), but can also sit on one of the surfaces (peripheral proteins). The peripheral proteins can slide around the membrane very quickly and collide with each other, but can never flip from one side to the other. The extracellular surface of the cell membrane is decorated

with carbohydrate groups attached to lipids, glycolipids, or proteins, glycoproteins. These short carbohydrates, or oligosaccharides, are usually chains of 15 or fewer sugar molecules. Oligosaccharides give a cell identity (i.e., distinguishing self from non-self) and are the distinguishing factor in human blood types and transplant rejection. A very significant chemical fact about membranes is that the relative proportion of protein differs greatly from lipids, ranging from 20% protein in the case of neuronal myelin membranes to 75% protein for the inner membrane of mitochondria [18].

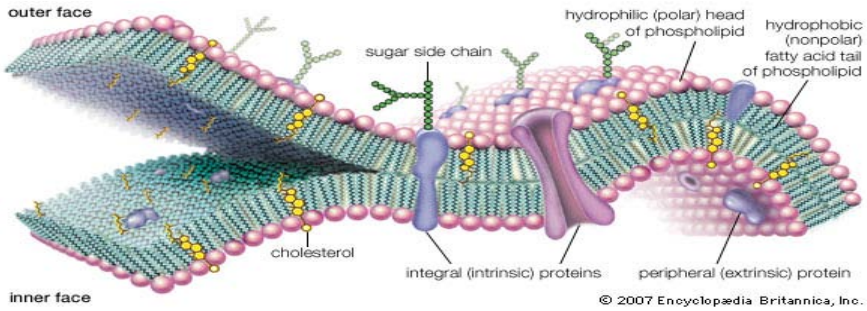

Figure 1-1: A molecular view of the cell membrane[1]

1.3.1 Lipids

Lipids may be broadly defined as hydrophobic or amphiphilic small molecules. In most membranes, approximately 40%-50% of the mass of the membrane is composed of lipids. Lipids provide a matrix for protein groups, acts as a barrier for ions & molecules and have the same structure in all membranes. Lipids are a diverse group of large biological molecules that do not include polymers and is made up primarily or exclusively of non-polar groups. They are grouped together and have little or no affinity for water. Due to their non-polar character, lipids typically dissolve more readily in non-polar solvents such as acetone, ether, and benzene etc. This solubility characteristic is of extreme importance in cells because lipids act as barriers and form

[1] Encyclopedia Britannica, Inc.

boundaries between and within cells. The hydrophobic behavior of lipids is based on their molecular structure. Although they have some polar bonds associated with oxygen, lipids consist mostly of hydrocarbons. Lipids link covalently with carbohydrates to form glycolipids and with proteins to form lipoproteins. Biological lipids originate entirely or in part from two distinct types of biochemical subunits or "building blocks": ketoacyl and isoprene groups [19]. Lipids can be divided into eight categories: fatty acyls, glycerolipids, phospholipids, sphingolipids, saccharolipids and polyketides (derived from condensation of ketoacyl subunits); and sterol lipids and prenol lipids (derived from condensation of isoprene subunits). However the major part of the cell membrane is constituted of phospholipids.

1.3.2 Phospholipids

Phospholipids are a class of lipids and are a major component of all cell membranes. Most phospholipids contain a diglyceride, a phosphate group, and a simple organic molecule such as choline. They are similar to fats, but have only two fatty-acids rather than three (see Fig 1-2).

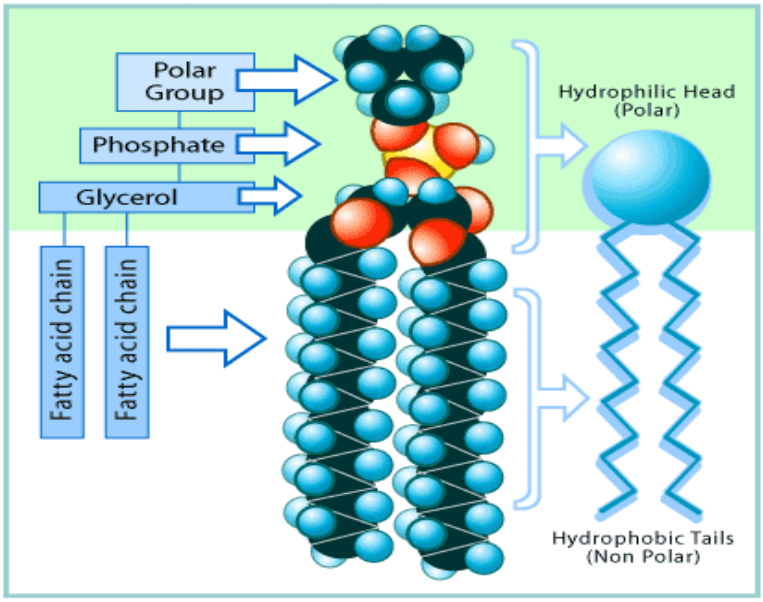

Figure 1-2: A Phospholipid molecule[2]

[2] snapshot taken from Inex Pharmaceuticals Corporation

The third hydroxyl group is joined to a phosphate group, which is negative in electrical charge and is therefore soluble in water. Phospholipids are described as amphipathic (or amphiphilic) molecules, having both a hydrophobic and a hydrophilic region. The two fatty acid tails which consist of hydrocarbons are hydrophobic and are excluded from water. Their heads, however which consist of the phosphate group and its attachments, are hydrophilic and have an affinity for water. Since the two fatty-acid chains are insoluble in water (hydrophobic), they are thought to project from the glycerol chain in a direction opposite to that taken by a polar group. When many phospholipid molecules are placed in water, their hydrophilic heads tend to face water and the hydrophobic tails are forced to stick together, forming a bilayer (see Fig 1-3)

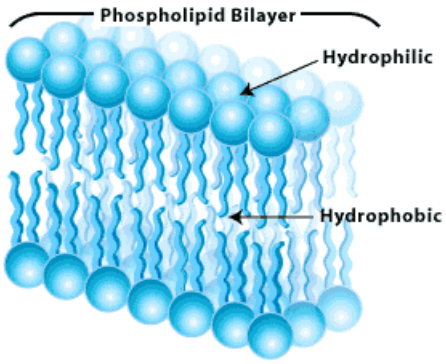

Figure 1-3: Schematic representation of a phospholipid bilayer[3]

The phospholipids differ among themselves in the identity of the fatty acids or of the polar group or both. In phosphoglycerides, a principal class of phospholipids, glycerol forms the backbone of the molecule, two fatty acid chains are esterified to two of the three hydroxyl groups in glycerol, and the third hydroxyl group is esterified to phosphate (see Fig 1-5a). The phosphate group can also be esterified to a hydroxyl group on another hydrophilic compound, such as serine, ethanolamine, choline, glycerol, and the inositol. The structural formulas of phosphatidyl choline and the other principal phosphoglycerides—namely, phosphatidyl ethanolamine,

[3] snapshot taken from Inex Pharmaceuticals Corporation

phosphatidyl serine, phosphatidyl inositol, and diphosphatidyl glycerol are shown in Fig 1-4. The second major class of membrane lipids are that of glycolipids; these are based on the molecule *sphingosine* (see Fig 1.5c). Though they possess the basic tuning-fork design of the phosphoglyceride they differ from them in several ways. The first long chain component is always a 15:1 hydrocarbon, which moreover, is linked to the base by a simple carbon-carbon bond rather than the ester bond (-COO-) found in the phosphoglycerides. In addition, a hydroxyl group is retained. *Sphingomyelin*, a phospholipid that lacks a glycerol backbone, is found mainly in plasma membranes (see Fig 1.5b). Instead of a glycerol backbone, it contains *sphingosine*, an amino alcohol with a long unsaturated hydrocarbon chain. In *sphingomyelin*, the hydrophilic head is similar to that of phosphatidylcholine. In Figure 1.5 the hydrophobic portions of all

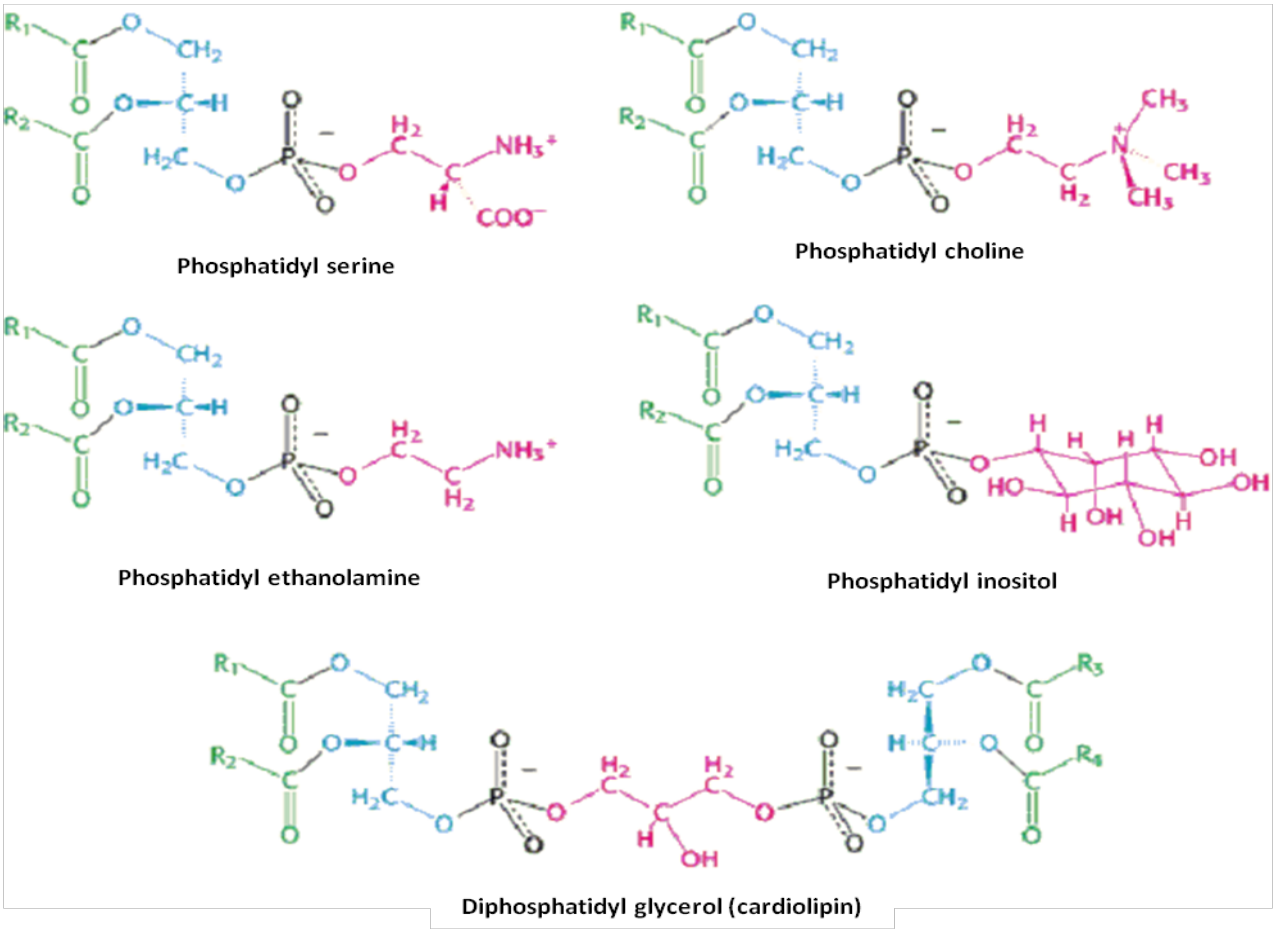

Figure 1-4: Some common phosphoglycerides found in memebranes

molecules are shown in yellow; the hydrophilic, in green. (a) Phosphatidylcholine is a typical phosphoglyceride. The fatty acyl side chains can be saturated, or they can contain one or more double bonds. (b) Sphingomyelin is a group of phospholipids that lack a glycerol backbone; a sphingomyelin may contain a different fatty acyl side chain than oleic acid (shown here). Linkage of sphingosine (outlined by black dots) to a fatty acid via an amide bond forms a ceramide. (c) Glucosylcerebroside, one of the simplest glycolipids, consists of the ceramide formed from sphingosine and oleic acid linked to a single glucose residue. This glycolipid is abundant in the myelin.

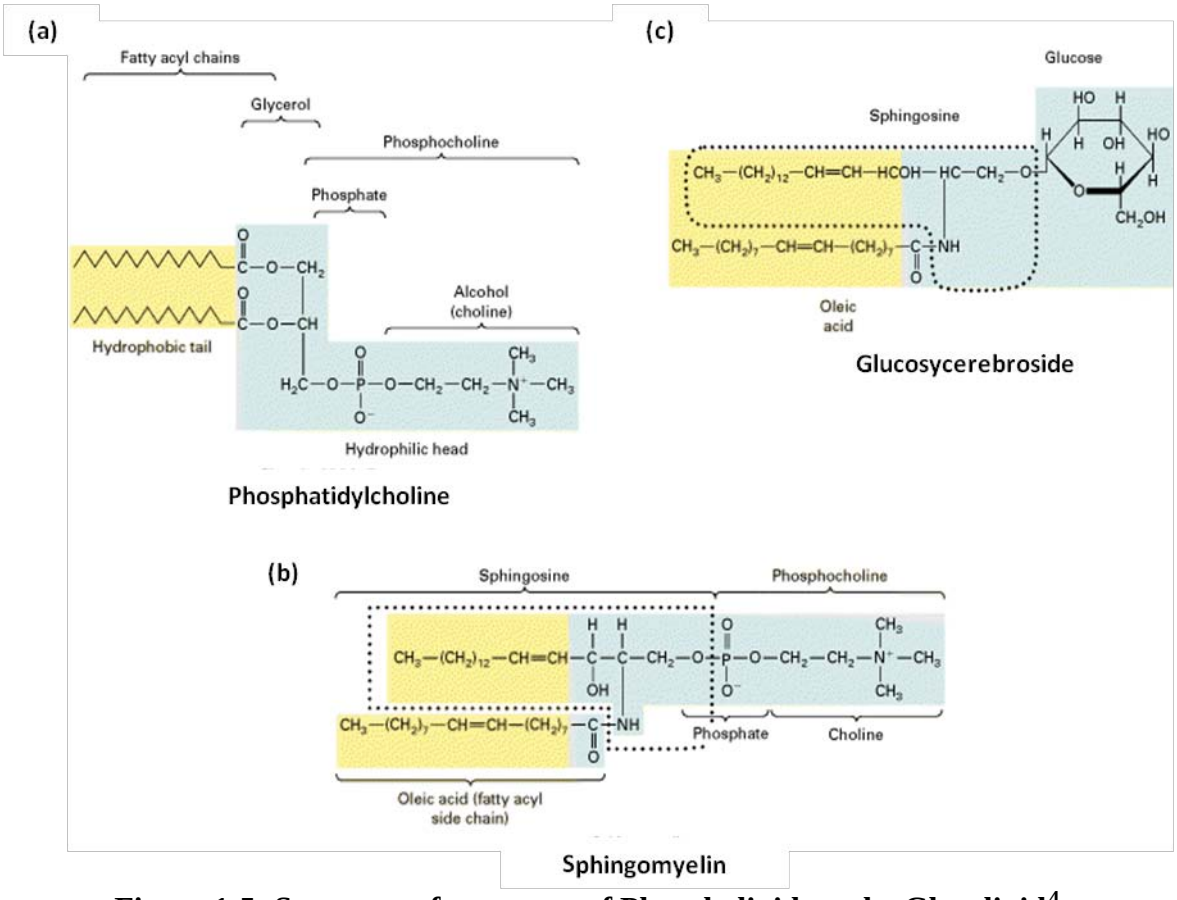

Figure 1-5: Structure of two types of Phospholipids and a Glycolipid[4].

The properties of a phospholipid are characterized by the properties of the fatty acid chain and the phosphate/amino alcohol. The long hydrocarbon chains of the fatty acids are of

[4] Lodish et al 2000

course non-polar. The phosphate group has a negatively charged oxygen and a positively charged nitrogen to make this group ionic. In addition there are other oxygen of the ester groups, which make on whole end of the molecule strongly ionic and polar.

Phospholipids when placed in an aqueous solution, due to its hydrophilic polar head group and hydrophobic tail its molecules will tend to arrange themselves in such a way that the hydrophilic heads will remain in contact with the water molecules, while the hydrophobic tails will orient themselves toward non-polar space, like air, other tails or the container. Most commonly, the phospholipids molecules will tend to arrange themselves in a double layer (bilayer sheet) (see Figure 1.6), both of whose surfaces will consist of heads, with their tails facing each other inside the bilayer membrane.

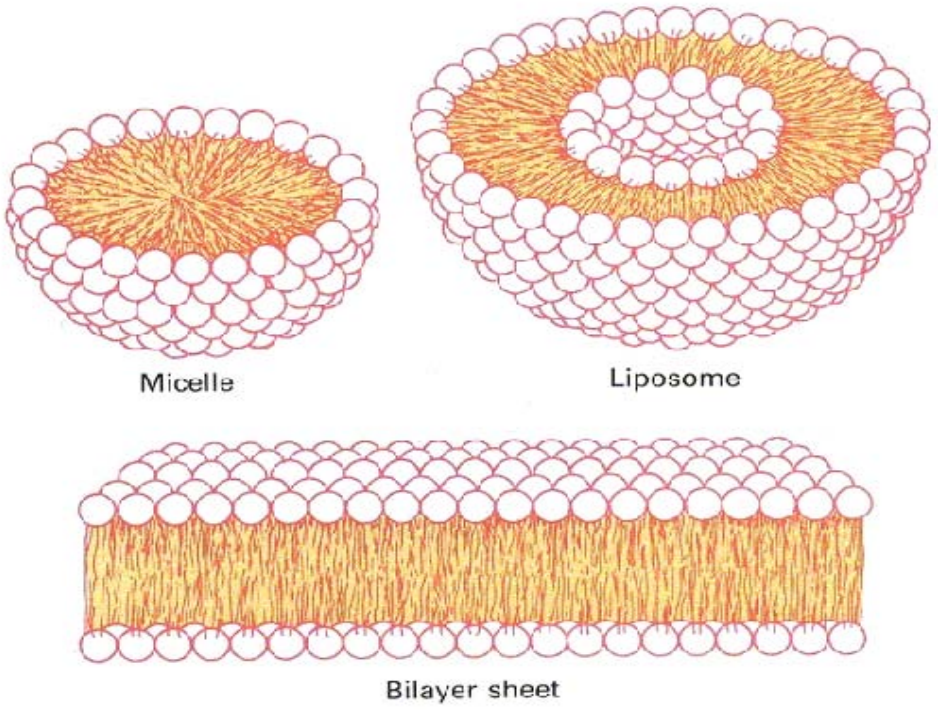

Figure 1-6: Cross sectional view of self-assembled lipid structures in water such as micelles, liposomes, and bilayer membranes[5]

[5] Snapshot taken from lamp.tu-graz.ac.at/~hadley/nanoscience/week4/assemble.gif

Under certain circumstances such as lipid concentration and solvent quality there is difficulty in filling all the volume of the interior of a bilayer, while accommodating the area per head group forced on the molecule by the hydration of the lipid head group leads to the formation tiny *spheroidal micelles* (see Figure 1.6), with the hydrophilic head regions in contact with surrounding solvent, sequestering the hydrophobic single tail regions in the micelle centre. If amphipathic lipids in high concentration are agitated in an acqueous suspension they form *spherical liposomes* (see Figure 1.6).

The basic physics had already been worked out by physicists such as Irving Langmuir [20], and Evert Gorter et al [21] and showed that bilayer was simply the most efficient (and therefore the most probable) way for phospholipid molecules to arrange themselves consistent with minimization of free energy So, in our study we considered phospholipids in the form of a bilayer and approximated it as a cell membrane.

1.3.3 Transport Mechanisms Across Cell Membranes

An important function of a biological membrane is to serve as a barrier to the outside world; it prevents items from coming into the cell and prevents the cell interior from leaking out of the cell. However, membranes are not impenetrable walls. Obviously, nutrients must enter the cell and waste products have to leave in order for the cell to survive. For this and many other reasons, it is crucial that membranes be selectively permeable. For example, the movement of ions across membranes is important in regulating vital cell characteristics such as cellular pH and osmotic pressure. Membrane permeability is also a key determinant in the effectiveness of drug absorption, distribution, and elimination. A membrane permits small hydrophobic molecules to readily pass back and forth across the membrane (lipids) but presents a formidable barrier to larger and more hydrophilic molecules (such as ions). These substances must be transported across the membrane by special proteins. We will look briefly at the three major ways that both

small hydrophobic molecules and hydrophilic molecules (such as ions) cross the barriers presented by cell membranes.

1.3.3.1 Diffusion Across the Lipid Bilayers

Since membranes are held together by weak forces, certain molecules can slip between the lipids in the bilayer and cross from one side to the other. This spontaneous process is termed diffusional bilayer crossing (Fig.1-7). This process allows molecules that are small and lipophilic (lipid-soluble), including small uncharged polar molecules such as water, urea, carbon dioxide, methanol, dimethylsulfoxide, glycerol, ethanol and non-polar molecules such as oxygen, nitrogen and most drugs rapidly penetrate through the bilayer [22]. This diffusion through the bilayer is a passive diffusion process where no energy is involved and substances are moved down the concentration gradient (Fick's Law). The rate of diffusion is increased by increasing the concentration difference, the surface area and membrane permeability. Lipid bilayers are much less permeable to larger polar molecules, and are virtually impermeable to ions, which are surrounded by a cage of water.

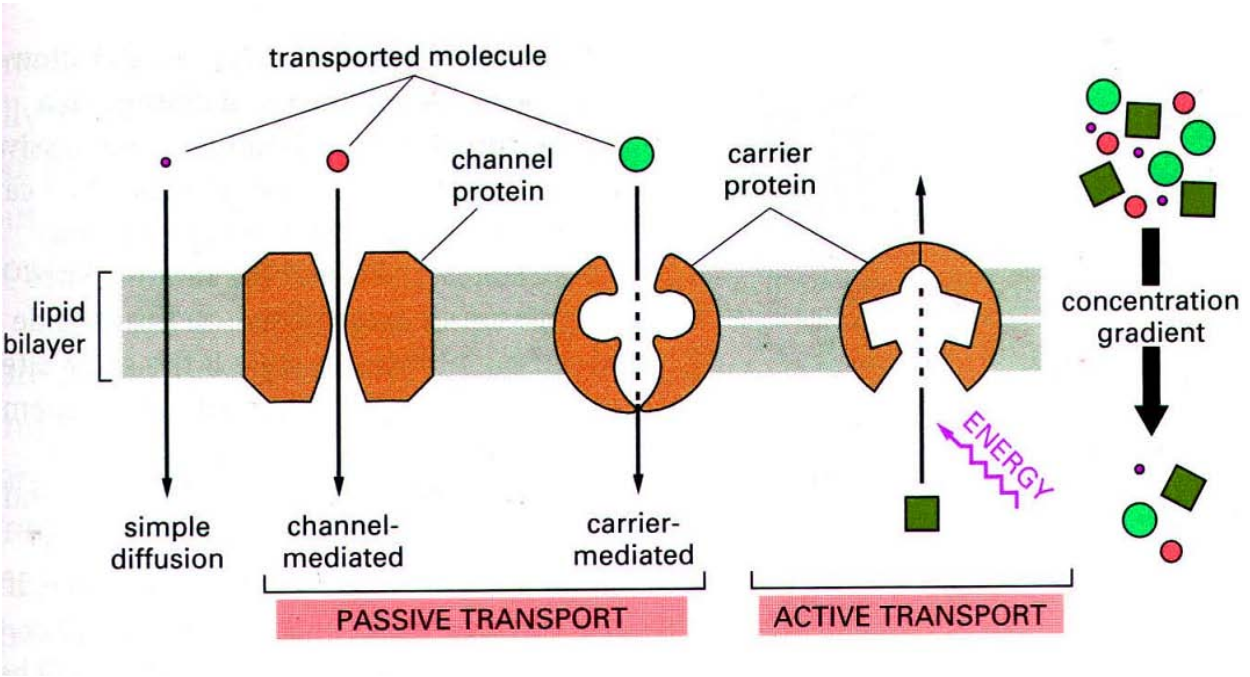

Figure 1-7: Transportation Phenomenon in Cell Membrane

1.3.3.2 Protein-Mediated Transport

In order to cross the hydrophobic interior of the bilayer, water-soluble molecules (those that are either charged or have polar groups) and large molecules require the action of membrane transport proteins. These integral membrane proteins provide a continuous protein-lined pathway through the bilayer. There are two classes of membrane transport proteins that we will discuss: carrier proteins, which literally carry specific molecules across, and channel proteins, which form a narrow pore through which ions can pass (Fig. 1-7). Channel proteins carry out passive transport [23], in which ions travel spontaneously down their gradients. Some carrier proteins mediate passive transport (also called facilitated diffusion), while others can be coupled to a source of energy to carry out active transport, in which a molecule is transported against its concentration gradient (Fig. 1-7).

1.3.3.3 Endocytosis/ Exocytosis

Large macromolecules (e.g., proteins, viruses, lipoprotein particles) require more complex mechanisms to traverse membranes, and are transported into and out of cells selectively via endocytosis and exocytosis (secretion). Interestingly, endocytosis and exocytosis are not only important for the import/export of large molecules. Often, essential small molecules that are hydrophobic or toxic (e.g., iron) travel through the bloodstream bound to proteins, which enter and exit cells via these mechanisms.

Although water is a polar molecule it has an unusual behavior, it can cross the bilayer rapidly, passing through a phospholipid bilayer in about a millisecond. Water molecules also move more rapidly through phospholipids bilayer than do substances that are dissolved in it. Water molecules move through the membranes at about 10^5 times faster than that of glucose molecules and 10^{10} times faster than that that of Na+ and K+ ions. We can get an idea of just

how fast water can pass across membranes into cells by watching how quickly red blood cells burst when put into water, or by noticing how quickly the leaves of a wilting plant regain their stiffness when placed in a vase of water. The reasons for this rapid movement of water might be because of its small size, its abundant concentration contents, and its dipolar nature which helps it to cross the charged lipid head group region. Though the exact reason is not known water does dissolve to a very slight extent in the hydrophobic core region. This helps us to make a hypothesis that a change in water concentration on one side of the bilayer should result in a rapid flow of water across the membrane.

1.3.4 Cryoprotectants

A cryoprotectant is a substance that is used to protect biological tissue from cell damage during freezing and thawing processes. It is extremely rare for cells to survive freezing and thawing without the presence of some type of cryoprotective agents (CPAs). Some cryoprotectants function by lowering a solution's or a material's glass transition temperature. In this way, the cryoprotectants prevent actual freezing, and the solution maintains some flexibility in a glassy phase. Many cryoprotectants also function by forming hydrogen bonds with biological molecules as water molecules are displaced. Hydrogen bonding in aqueous solutions is important for proper protein and DNA function. Thus, as the cryoprotectant replaces the water molecules, the biological material retains its native physiological structure (and function), although they are no longer immersed in an aqueous environment. This preservation strategy is most often observed in anhydrobiosis. Some of the common cryoprotective agents used are dimethylsulfoxide (DMSO), ethylene glycol, glycerol, propylene glycol, sucrose and trehalose. Glycerol and dimethylsulfoxide have been used for decades by cryobiologists to reduce ice formation in cells that are cold-preserved in liquid nitrogen. In most cases these compounds must

penetrate through the cell membrane in order to exert their protective effect. Passive transport of water and cryoprotective solutes across the membranes of individual cells plays an absolutely important role in low temperature biology (cryopreservation), since low temperatures tend to diminish the relative importance of active transport processes. So cryopreservation requires an understanding of passive transport of cryoprotectant and water across the cell membrane. Due to the wide use of DMSO as cryoprotectant, in this study we have primarily focused on the passive transport of water and DMSO across the cell membrane.

1.3.4.1 Dimethylsulfoxide (DMSO)

DMSO ($(CH3)_2SO$) is a polar aprotic solvent that dissolves both polar and nonpolar compounds and is miscible in a wide range of organic solvents as well as water. It has wide applications in organic chemistry, chemical technology, cell biology and medicine because of its many important biological properties. DMSO is able to induce cell fusion [24] cell differentiation [25] increase permeability across membrane [26, 27] and to change properties of proteins [28]. The cryoprotective property of DMSO was discovered more than 50 years ago by Lovelock and Bishop [29] and concentrations up to 40% are used in cryopreservation of wide variety of cells [30, 31]. Several experimental studies had also investigated the effect of DMSO on the structure of the model cell membranes [32-39]. Most of these studies have used either a differential scanning calorimeter or an X-ray diffraction to probe the effect of DMSO on lipid bilayer. Tristram-Nagle et al [33] and Chang and Dea [32] studied the effect of DMSO on the phase transition of phospholipid bilayers and concluded that the presence of DMSO effects the solvation of phospholipid bilayers. DMSO also has a significant effect on thickness of the bilayer [35], and modifies the hydration forces [34]. However, the molecular mechanisms involved in DMSO-lipids (cell membrane) are still being studied.

Recent advances in computational resources have permitted large scale molecular dynamic simulations for studying the interactions of different chemicals on lipid bilayers at molecular level. With computer simulations we can analyze biomembrane properties from atomistic perspective with a degree of detail that is hard to reach by other techniques. The excellent agreement of the results obtained with various molecular dynamics (MD) studies [40, 41] on simple model membranes with experiments, has raised the confidence in applying the atomistic simulations to even more complex systems. Although numerous MD simulations have been done to study the interaction of various small molecules on lipid bilayers [27, 41-53], only few computational studies of DMSO have appeared in literature. Paci and Marchi [52] was one of the early studies to study the permeability of glycerolipid bilayer to a polar DMSO molecule. To obtain more detailed information of DMSO/phospholipid, Smondyrev and Berkowitz [49] studied the properties of lipid bilayers in presence of pure DMSO for time scale of the order of 2ns. They have concluded that there is no larger penetration of DMSO molecules into the membrane and there is no change in the area per lipid. In contrary, Sum and de Pablo [51] showed that DMSO increases the area per lipid and it penetrates much deeper into the bilayer than water. They studied the effect of different concentrations of DMSO at different temperatures, on the structure of the phospholipid bilayer for a time scale of 10 ns. Although, these MD simulations have shed considerable light on the interactions between DMSO and lipid bilayers, the total simulation time which was less than 10ns which very short time for system to to reach the equilibrium state. Recent simulations by Moldovan et al [27] and Gurtovenko et al [47] showed that higher concentrations of DMSO leads to pore formation in the bilayers even without the presence of any external forces such as stresses or forces generated by high electric fields. Gurtovenko et al studied the effect of different concentrations of DMSO ranging from 0%

to 100% on dipalmitoylphosphatidylcholine (DPPC) on simulations spanning 30ns in total time. Their study showed that at low concentrations of DMSO(<10mol%), DMSO induced membrane expansion which leads to decrease in membrane thickness and concentration of 10mol%-20mol% leads to pore formation and further more increase in concentration leads to disintegration of membrane. Despite the advances in this area there are still important unanswered questions regarding the effects of DMSO on stability and structural characteristics of lipid bilayers.

1.4 Objectives of the Present Work

The objective of the present work is to advance the fundamental understanding of the effect of low and moderate concentrations of DMSO on lipid bilayers. To reach our objective we:

- Performed atomistic simulations of phospholipid bilayers in the presence of water and DMSO solutions at various concentrations.
- Investigated the bilayer stability and structural characteristics when exposed to both symmetric and asymmetric water/DMSO solutions.
- Investigated the effect of DMSO on lipid bilayers line tension.
- Investigate the effect of DMSO on growth kinetics of preexisting pores in lipid bilayers.

2 MOLECULAR DYNAMICS SIMULATION METHODOLOGY

2.1 Simulations Vs Experiments

Due to the advancements in computational hardware and simulation programs, computer simulations play a vital role in science today. In the past, physical sciences were characterized by interplay between experiment and theory. In experiment, a system is subjected to measurements, and results are obtained in numeric form. In theory, a model is constructed and is then validated by its ability to describe the system behavior in a few selected cases, simple enough to allow the solution to be computed. In many cases, under 'special circumstances' this implies a considerable amount of simplification in order to eliminate all the complexities invariably associated with real world problems. Unfortunately, many physical problems of extreme interest fall outside the realm of these 'special circumstances'. Among them, one could mention the physics and chemistry of defects, clusters of atoms, surfaces, biological macromolecules etc. which involve a large amount of degrees of freedom, and require an accurate treatment of temperature effects and phase transitions.

The development of high speed computers has inserted a new element right in between experiment and theory: the *computer simulations*. In a computer simulation a model is still provided by theorists, but the calculations are performed by the machine following a recipe (the algorithm, implemented in a suitable programming language). In this way complexity can be increased and more realistic systems can be investigated, opening a road towards a better understanding of real experiments. Computer simulations increased the demand for accuracy of the models. For instance, a molecular dynamics simulation allows to study the mobility of grain boundaries of a material, modeled by means of a certain interaction law. This is a difficult test for the theoretical model to pass- and a test which has not been available in the past. Therefore,

simulation ‘brings to life’ the models, disclosing critical areas and providing suggestions to improve them which is not possible by theoretical models. Computer simulations can often come very close to experimental conditions, to the extent that computer results can sometimes be compared directly with experimental results. When this happens, computer simulations become an extremely powerful tool not only to understand and interpret the experiments at microscopic level, but also to study regions which are not accessible experimentally or which would imply very expensive experiments.

Computer simulations deal with models not with the ‘real thing’: this suggests classifying simulation as belonging to theoretical methods without hesitation. But it also involves performing runs, and analyzing which pretty much makes it to resemble to experiments quite closely. It is important to realize that simulation increases the threshold of complexity which separates ‘solvable’ and ‘unsolvable’ models. We can take advantage of this threshold and move up one level in our description of physical systems. This gives us an additional degree of freedom to explore new possibilities. Transportation of water & cryoprotectant molecules has been studied extensively by phenomological models. However although these models are powerful tools in predicting macroscopic phenomenons they do not bring any insights and understanding into the detailed microscopic mechanisms of transport across membranes. So to obtain the detailed insights of the phenomena at microscopic level we chose to apply “*Molecular Dynamic simulation*” methodology for our study.

2.2 Molecular Dynamic Simulation

The concept of Molecular Dynamics (MD) simulation was originally developed by Alder & Wainwright in the early 1950’s [54] who studied a system of colliding hard core particles. The next major advance was in 1964, when Rahman carried out the first simulation using a realistic

potential for liquid argon [55]. The first molecular dynamics simulation of a realistic system was done by Rahman and Stillinger in their simulation of liquid water in 1974 [56]. The underlying idea behind 'Molecular Dynamics Simulations' is that we can study the average behavior of a many-particle system simply by computing the natural time evolution of the system numerically, by integrating their equations of motion and averaging the quantity of interest over a sufficiently long time. MD represents an interface between laboratory experiments and theory, and can be understood as a "virtual experiment".

Molecular dynamics is a specialized discipline of molecular modeling and computer simulation based on statistical mechanics; the main justification of the MD method is that statistical ensemble averages are equal to time averages of the system, known as the ergodic hypothesis. MD has also been termed as "statistical mechanics by numbers" and "Laplace's vision of Newtonian mechanics", predicting the future by animating nature's force (references from Wikipedia) and allowing insight into molecular motion on an atomic scale. In MD simulations we try to reproduce the time development of a system with N interacting atoms with masses m_i by directly solving Newton's equation of motion,

$$F_i = m\frac{d^2 r_i}{dt^2} \tag{2.1}$$

Where r_i is the position of the particle i at time t. The momentary force F_i on each atom can be calculated from the interactions occurring between the atoms in the system. The force F_i acting on each particle in the system can be calculated as the negative gradient of the potential energy function (V) which in turn is a function of the atom coordinates.

$$F_i = \nabla_{r_i} V(r_1, r_2 \ldots \ldots r_N) \tag{2.2}$$

The calculation of this potential function is a central part of the algorithm.

2.2.1 Potential Energy Function

Potential function is calculated as a sum of internal, or bonded, terms V_{bonded} , which describe the bonds, angles and bond rotations in a molecule, and a sum of external or nonbonded terms, $V_{non-bonded}$, These terms account for interactions between nonbonded atoms or atoms separated by 3 or more covalent bonds (Lennard-Jones interactions and electrostatic interactions).

$$V(r) = V_{bonded} + V_{non-bonded} \tag{2.3}$$

$$V_{bonded} = V_{bond-stretch} + V_{angle-bend} + V_{rotate-along-bond} \tag{2.4}$$

The first term in the above equation is a harmonic potential representing the interaction between atomic pairs where atoms are separated by one covalent bond, i.e., 1, 2-pairs. This is the approximation to the potential of atoms i and j joined by a covalent bond as a function of displacement from the ideal bond length.

$$V_{bond-stretch} = \sum_{1,2\ pairs} K_{ij}\left(r_{ij} - r_{ij}^{0}\right)^{2} \tag{2.5}$$

Where K_{ij} is a force constant that describes the strength of the actual type of bond and r_{ij}^{0} is the equilibrium length of the bond. Both equilibrium length of the bond and force constant are specific for each pair of bound atoms, i.e. depend on the chemical type of the atom constituents. Values of force constant are often evaluated from experimental data such as infrared stretching frequencies or from quantum mechanical calculations. Values of bond length can be inferred from high resolution crystal structures or microwave spectroscopy data.

The second term in above equation is associated with alteration of bond angles theta from ideal values θ_{ijk}^{0}, for the atoms i, j, k (where i, j, k are bonded together with i bonded with

j and j bonded with k) can be described by harmonic potential function,

$$V_{bond-angle} = \sum_{angles} K_{ijk}\left(\theta_{ijk} - \theta^{0}_{ijk}\right)^{2} \quad (2.6)$$

The force constant K_{ijk} determines how hard it is to distort the angle. Values of θ^{0}_{ijk} and K_{ijk} depend on chemical type of atoms constituting the angle.

The third term represents the torsion angle potential function which models the presence of steric barriers between atoms separated by 3 covalent bonds (1,4 pairs). The motion associated with this term is a rotation, described by a dihedral angle and coefficient of symmetry *n=1,2,3*), around the middle bond. This potential is assumed to be periodic and is often expressed as a cosine function.

$$V_{rotate-along-bond} = \sum_{1,4\ pairs} K_{ijkl}\left(1 - \cos[(n\emptyset))]\right] \quad (2.7)$$

with K_{ijkl} being the force constant that describes the strength required to distort the dihedral angle formed between four bonded atoms.

The Potential term representing the contribution of non-bonded interactions in the total potential function (Eq 2.3) has two components, the Van der Waals interaction energy and the electrostatic interaction energy. The nonbonded interactions are computed on the basis of a neighbor list (a list of non-bonded atoms within a certain radius), in which exclusions are already removed. In the potential energy function, these interactions are accounted by the electrostatic and Van der Waals interactions.

$$V_{non-bonded} = V_{Van\ der\ waals} + V_{elctrostatic} \quad (2.8)$$

The van der Waals interaction between two atoms arises from a balance between repulsive and attractive forces. The repulsive force arises at short distances where the electron-electron

interaction is strong. The attractive force, also referred to as the dispersion force, arises from fluctuations in the charge distribution in the electron clouds. The van der Waals interaction is most often modeled using the Lennard-Jones 6-12 potential which expresses the interaction energy using the atom-type dependent constants A_{ij} and B_{ij}. Values of A_{ij} and B_{ij} may be determined by a variety of methods, like non-bonding distances in crystals and gas-phase scattering measurements**.**

$$V_{Van\ der\ waals} = \sum_{\substack{nonbonded \\ pairs}} \left(\frac{A_{ij}}{r_{ij}^{12}} - \frac{B_{ij}}{r_{ij}^{6}} \right) \tag{2.9}$$

The electrostatic interaction between a pair of atoms is described by Coulomb term,

$$V_{electrostatic} = \sum_{\substack{nonbonded \\ pairs}} \frac{q_i q_j}{4\pi\varepsilon_o \varepsilon_r r_{ij}} \tag{2.10}$$

Where q_i and q_j are the charges. The permittivity of free space is designated by ε_o and ε_r is the relative permittivity. The distance between the atoms is denoted by r_{ij}.

The empirical potential energy function is differentiable with respect to the atomic coordinates; this gives the value and the direction of the force acting on an atom and thus it can be used in a molecular dynamics simulation. The calculation of force results in the calculation of the acceleration which tells us how the speed is changing, and from the speed variation it is possible to determine approximate positions of the atoms a very short time later. This process is called integrating equations of motion, and repeating calculation for huge number of small steps results in a trajectory with the development of positions, velocities and forces on all atoms during the simulation. A good approximation of the potential function would provide an extremely

detailed description of both dynamics and equilibrium properties in the system under study.

2.2.1.1 Limitations in Calculating Potential Energy Function

The empirical potential function has several limitations, which result in inaccuracies in the calculated potential energy.

One limitation is due to the fixed set of atom types employed when determining the parameters for the force field. Atom types are used to define an atom in a particular bonding situation, for example an aliphatic carbon atom in a sp^3 bonding situation has different properties than a carbon atom found in the benzene ring. Instead of presenting each atom in the molecule as a unique one described by unique set of parameters, there is certain amounts of grouping in order minimize the number of atom types. This can lead to type-specific errors. The properties of certain atoms, like aliphatic carbon or hydrogen atoms, are less sensitive to their surroundings and a single set of parameters may work quite well, while other atoms like oxygen and nitrogen are much more influenced by their neighboring atoms. These atoms require more types and parameters to account for the different bonding environments.

An approximation introduced to decrease the computational demand is the pair-wise additive approximation, i.e., interaction energy between one atom and the rest of the system is calculated as a sum of pair-wise (one atom to one atom) interactions, or as if the pair of atoms do not see the other atoms in the system. The simultaneous interaction between three or more atoms is not calculated, so certain polarization effects are not explicitly included in the force field. This can lead to subtle differences between calculated and experimental results.

Another important point to take into consideration is that the potential energy function does not include entropic effects. Thus, a minimum value of V calculated as a sum of potential functions does not necessarily correspond to the equilibrium, or the most probable state; this

corresponds to the minimum of free energy. Because of the fact that experiments are generally carried out under isothermal-isobaric conditions (constant pressure, constant system size and constant temperature) the equilibrium state corresponds to the minimum of Gibb's Free Energy, *G*. While just an energy calculation ignores entropic effects, these are included in molecular dynamics simulations.

2.2.2 Integration Algorithms

The potential energy is a function of the atomic positions (3N) of all the atoms in the system. Due to the complicated nature of this function, there is no analytical solution to the equations of motion; they must be solved numerically. In order to get a solution as accurate as possible, a high accuracy time integration algorithm to integrate Eq. 2.1 with small steps would be very much necessary [57, 58]. It does not matter how often the forces had to be calculated. The situation in macromolecular systems usually studied with molecular dynamics is however very different. In this case it is unnecessary to determine a very detailed solution for individual atoms since in the dynamics; small numerical errors will grow exponentially and affect the trajectories. This might strike bad at first since it affects the whole concept of simulations, but it only reflects real systems-equilibrium properties are not sensitive to details of individual trajectories. It is thus fruitless to reproduce motions exactly. Instead, one should make sure that any reasonably long part extracted from a trajectory would be a fair description of a particle with the same initial conditions Lindahl, 2001 [58].

Numerous numerical algorithms have been developed for integrating the equations of motion. These include:

- Verlet algorithm
- Leap-frog algorithm

- Velocity Verlet algorithm
- Beeman's algorithm

All the integration algorithms assume that the positions, velocities and accelerations can be approximated by a Taylor series expression:

$$r(t+\delta t) = r(t) + v(t)\delta t + \frac{1}{2}a(t)\delta t^2 + \cdots \quad (2.11)$$

$$v(t+\delta t) = v(t) + a(t)\delta t + \frac{1}{2}b(t)\delta t^2 + \cdots \quad (2.12)$$

$$a(t+\delta t) = a(t) + b(t)\delta t + \cdots \quad (2.13)$$

Where r is the position, v is the velocity (the first derivative of position with respect to time), a is the acceleration (the second derivative of position with respect to time), and b is the third derivative of position with time.

2.2.2.1 Verlet Algorithm

Verlet algorithm is one of the most commonly used algorithms developed by Verlet [59]. The Verlet algorithm uses positions and accelerations at time *t* and the positions from time $t-\delta t$ to calculate new positions at time $t+\delta t$.

$$r(t+\delta t) = r(t) + v(t)\delta t + \frac{1}{2}a(t)\delta t^2 + \cdots \quad (2.14)$$

$$r(t-\delta t) = r(t) - v(t)\delta t + \frac{1}{2}a(t)\delta t^2 + \cdots \quad (2.15)$$

Summing Eq. 2.14 and Eq. 2.15 we get

$$r(t+\delta t) = 2r(t) - r(t-\delta t) + a(t)\delta t^2 + \cdots \quad (2.16)$$

This offers an advantage that the first and third-order term from the Taylor expression cancels out, thus making the Verlet algorithm more accurate than integration Taylor expansion alone.

Note that if using this equation at $t = 0$, one needs the position at time $-\delta t$, $r(-\delta t)$. At first sight this could cause problems, because the initial conditions are known only at the initial time. This can be solved by doing the first time step using the equation

$$r(\delta t) \approx r(0) + v(0)\delta t + \frac{1}{2}a(0)\delta t^2 + \cdots \tag{2.17}$$

The advantages of the Verlet algorithm are, i) it is straightforward, and ii) the storage requirements are modest. The disadvantage is that the algorithm is of moderate precision.

2.2.2.2 Leap-Frog Algorithm

A slightly modified, but theoretically equivalent, algorithm is the Leap-Frog algorithm [60] which handles velocities somewhat better than Verlet Algorithm. In this algorithm, the velocities are first calculated at time $\left(t + \frac{\delta t}{2}\right)$; these are used to calculate the positions, *r*, at time $(t + \delta t)$. In this way, the velocities *leap* over the positions, then the positions *leap* over the velocities. The Leap-Frog algorithm is not self-starting. The current state and a prior state must both be known to advance the solution. Since the prior state is not known for the initial conditions, a prior state is estimated when the initialize method is invoked.

$$r(t + \delta t) = r(t) + v\left(t + \frac{1}{2}\delta t\right)\delta t \tag{2.18}$$

$$v\left(t + \frac{1}{2}\delta t\right) = v\left(t - \frac{1}{2}\delta t\right) + a(t)\delta t \tag{2.19}$$

The advantage of this algorithm is that the velocities are explicitly calculated and it is much faster than Verlet algorithm, however the disadvantage is that they are not calculated at the same time as the positions. The velocities at time *t* can be approximated by the relationship:

$$v(t) = \frac{1}{2}\left[v\left(t + \frac{1}{2}\delta t\right) + v\left(t - \frac{1}{2}\delta t\right)\right] \tag{2.20}$$

2.2.2.3 Velocity Verlet Algorithm

Another commonly used algorithm is velocity Verlet algorithm; this uses a similar approach but explicitly incorporates velocity, solving the first-time step problem in the Basic Verlet algorithm:

$$r(t+\delta t) = r(t) + v(t)\delta t + \frac{1}{2}a(t)\delta t^2 \tag{2.21}$$

$$v(t+\delta t) = v(t) + \frac{1}{2}[a(t) + a(t+\delta t)]\delta t \tag{2.22}$$

The advantage of velocity algorithm is that it consumes less memory compared to Verlet algorithm.

2.2.2.4 Beeman's Algorithm

Beeman's algorithm is closely related to Verlet algorithm. It produces identical positions to Verlet, but is more accurate in velocities and gives better energy conservation.

$$r(t+\delta t) = r(t) + v(t)\delta t + \frac{2}{3}a(t)\delta t^2 - \frac{1}{6}a(t-\delta t)\delta t^2 \tag{2.23}$$

$$v(t+\delta t) = v(t) + v(t)\delta t + \frac{1}{3}a(t)\delta t + \frac{5}{6}a(t)\delta t - \frac{1}{6}a(t-\delta t)\delta t \tag{2.24}$$

The disadvantage is that the more complex expressions make the calculation more expensive.

2.2.3 Constraint Algorithms

Constraint algorithms are often applied to molecular dynamics simulations. Although such simulations are sometimes carried out in internal coordinates that automatically satisfy the bond-length and bond-angle constraints. To extend the length of the simulation we have to use a longer time step, but due to the increase in the time step there will be successively larger errors in the motions, and after a few steps the fluctuations will diverge, causing the whole simulation to crash. To solve these problems 'Constraint Dynamics' is often employed in the simulations. It completely removes the bond and/or angle degrees of freedom from the system. Explicit

constraint forces typically shorten the time-step significantly, making the simulation less efficient computationally; in other words, more computer power is required to compute a trajectory of a given length but avoids the errors when integrating bond oscillations. The constant bond lengths are also fairly good approximations of the ground states of quantum mechanical oscillators. Explicit constraint forces typically shorten the time-step significantly, making the simulation less efficient computationally; in other words, more computer power is required to compute a trajectory of a given length. Most commonly used constraint algorithms are:

- SHAKES Algorithm
- LINCS Algorithm

2.2.3.1 SHAKES Algorithm

The SHAKE algorithm was the first and most widespread algorithm developed to satisfy bond geometry constraints during molecular dynamics simulations. It solves the system of non-linear constraint equations using the Gauss-Seidel method to approximate the solution of the linear system of equations. In this algorithm for each pair of atoms involved in a bond (or triplet in an angle), force necessary to restore then to the equilibrium value, is calculated. In a macromolecular system since a lot of bonds are connected, the algorithm has to be iterated continuously until convergence is achieved. This limits the applicability somewhat; for time steps greater than 2-3 fs it does not always converge, and the iteration makes it unsuitable for parallel computers since it incurs a lot of extra communication between processors.

2.2.3.2 LINCS Algorithm

An alternative constraint method, LINCS (Linear Constraint Solver) was developed in 1997, but was based on earlier method, EEM [61], and a modification thereof [62]. This algorithm resets bonds to their correct lengths after an unconstrained update [63]. This is non-iterative approach, as it always uses two steps. This advantage makes it possible to extend time

steps at least to 3-4 fs. Although LINCS is based on matrices, no matrix-matrix multiplication is involved. LINCS has been reported to be 3-4 times faster than SHAKE [63], but it can only be used with bond constraints and isolated angle constraints.

2.2.4 Limitations of Molecular Dynamic Simulations

Although Molecular dynamic simulation is a powerful technique, it has number of limitations. Using Newton's equation implies the use of Classical mechanics to describe the motion of atoms, but it is known that systems at atomistic level obey quantum laws rather than classical laws. Therefore one cannot hope to describe chemical reactions in which bonds form or break by using classical MD method.

The accuracy of the simulation is entirely dependent on the accuracy of the underlying force field, which contains several approximations and various fitted parameters. The forces are usually obtained as the gradient of the potential energy function depending on the positions of the particles. The realism of the simulation is dependent on the ability of the chosen potential functions to reproduce the behavior of the system under the conditions at which the simulation is run. To speed up the calculation of forces, the non-bonded interactions are usually truncated beyond a distance of 1-2 nm. This is a fair approximation for Lennard-Jones interactions but not always for electrostatics if there are free charges in the system.

One of the limitations is choosing the maximum time step for which the integration of the equations of motion is still stable. A typical value in practice is 2 fs (10^{-15}s). This means that 500, 000 computationally expensive integration steps are necessary to calculate the dynamics of a system over 1 ns time period. If the system is composed of a large number of atoms, say a few tens of thousand atoms, this can take one to two weeks when run on a single processor computer. This limits the length of the current simulation to nanoseconds time scale. Molecular Dynamic

simulations can be performed on systems containing thousands or perhaps millions of atoms and for simulation times ranging from a few picoseconds to hundreds of nanoseconds. Though these numbers are certainly respectable, it may happen to run into conditions where time and size limitations become important. Despite, of all the limitations if the approximations are kept in mind and the results carefully checked, molecular dynamics is a very reliable method to study the motions present in biological macromolecules.

2.2.5 Software Packages Available for MD Simulations

AMBER: (Assisted Model Building using Energy Refinement)

A suite of programs for molecular mechanics and molecular dynamic simulations. Designed primarily for proteins and nucleic acids.

CHARMM: (Chemistry at HARvard, Macromolecular mechanics)

It is highly regarded and widely used simulation package. CHARMM combines standard minimization and dynamics capabilities with expert features including free energy perturbation (FEP), correlation analysis and combined quantum, and molecular mechanics (QM/MM) methods. Simulations provide insight into molecular-level structure, interactions, and energetics. It has been ported to numerous platforms in both serial and parallel architectures.

NAMD: (NAnoscale Molecular Dynamics)

It is a molecular dynamics simulation package written using the Charm++ parallel programming model, noted for its parallel efficiency and often used to simulate large systems (millions of atoms). NAMD uses the popular molecular graphics program VMD for simulation setup and trajectory analysis, but is also file-compatible with AMBER, CHARMM, and X-PLOR.

LAMMPS: (Large-scale Atomic/Molecular Massively Parallel Simulator)

LAMMPS makes use of MPI for parallel communication and is a free open-source code.

GROMACS: (GROningen MOlecular Simulation package)

GROMACS is a versatile package to perform molecular dynamics, i.e. simulate the Newtonian equations of motion for systems with hundreds to millions of particles. It is primarily designed for biochemical molecules like proteins and lipids that have a lot of complicated bonded interactions. GROMACS provides extremely high performance compared to all other programs. GROMACS can be run in parallel, using standard MPI communication.

2.3 Review of Literature

One of the great challenges in biology during the past decades is to understand the basic principles of biomembranes, which govern and mediate various biologically relevant processes at microscopic level. Studies of lipid bilayers that used as model systems for biological membranes have been the focus of research for a long time. Many experimental studies have provided abundant structural aspects of lipid bilayer systems. Neutron scattering [64], and X-ray diffraction [33, 64-67] are probably the most powerful experimental techniques to determine structure at atomistic level. Other experimental techniques include, NMR [68-71] infrared spectroscopy [72] DSC and fluorescence spectroscopy [73]. Though experimental approach is the cornerstone in membrane research it is often impossible to obtain all the atomistic details by experiments only. Computer simulations such as molecular dynamic simulations can assist in the understanding of the experiments, in part by providing the atomistic details that are experimentally unavailable or difficult to obtain [27, 40, 41, 74, 75].

The molecular dynamics study has developed over the decades from a method to study the dynamics of liquids of solid spheres and lennard-jones particles to the study of different types of systems at atomistic level. The development of particular use of molecular dynamics was greatly used in 1980's when a number of general purpose simulation computer programs became available, e.g. AMBER[76], CHARMM [77], GROMOS [78] and OPLS [79]. Initially many simulations of simple bilayer membrane model systems without solvent have been studied by van-der-Ploeg and Berendsen [80, 81]. Availability of powerful computers has opened new ways for researchers to replace these simple models by more sophisticated ones. The pioneering MD simulation study on dipalmitoylphosphatidylcholine DPPC/water binary system, as representative for a biological membrane was studied by Egberts in 1988 [82, 83]. In this study a simulation system which reproduced experimental results and which can serve as a starting point for future simulations incorporating other molecules was set up. These simulations provided a very detailed picture on a microscopic level of static arrangement and dynamic properties of the constituent molecules. It also provided an insight in the changes that occur at the main phase transition from gel to liquid crystalline state. Since then molecular dynamic simulations of biological membranes have come of age. The excellent agreement of the results obtained with various molecular dynamics (MD) studies on simple model membranes with experiments has raised the confidence in applying the atomistic simulations to even more complex systems. Membrane simulations have been reviewed several times during the 90's [41, 43, 45, 75, 84]. Increasing interest in performing such simulations encouraged researchers to perform simulations on a variety of lipid bilayer systems. Atomic level simulations of lipid bilayers of dipalmitoylphosphatidylcholine (DPPC) and other lipid bilayers have been carried out by several groups over the past several years [41, 42, 85-89]

Recent advances in processor speeds and the availability of parallel computers allowed major advances in increasing the length and time scales accessible to bilayer MD simulations. With the advent of increase in simulation duration, number of researchers started analyzing motions on the nanosecond time scales. Essman and Berkowitz [90] detailed the slow motion of PC head group atoms and found that a constant dipole potential is maintained in the membranes because the orientation of water molecules compensates for the headgroup fluctuations. Membrane simulations with durations of 10ns were reported by Feller and group [74] and Essman & Berkowitz [90]. Lindahl and Edholm [91] performed simulation on a very large system consisting of 1024 lipids and estimated the relaxation time of collective undulations and peristaltic modes of motion. Molecular dynamic simulations are well suited for detailed analysis of the interactions between lipid bilayers and various small molecules, including water, chemicals, co-enzymes, peptides and proteins, as evidenced by the extensive body of published literature [27, 37, 41-45, 47-53, 74, 75, 80, 81, 86, 88, 92-114]. Briefly these studies describe the effect of cholesterol [104, 105], of dimethylsulfoxide [27, 47-49, 51, 100, 101], of methanol [53], of ions [106, 107], and proteins [108, 109] on lipid bilayers; others describe the permeability coefficients of small organic molecules through lipid bilayer [48, 111], the permeation of water across a lipid bilayer [45, 98].

3 INVESTIGATION OF STRUCTURAL CHANGES IN LIPID BILAYERS INDUCED BY DIMETHYLSULFOXIDE: SYMMETRIC BILAYER SYSTEM

3.1 Introduction

The interaction of DMSO with lipid membranes and other biological macromolecules is a subject of interest due to both fundamental and biophysical questions of solvent-solute interactions. DMSO is an aprotic solvent that has wide applications in organic chemistry, chemical technology, cell biology and medicine because of its many important biological properties. DMSO is able to induce cell fusion [24] cell differentiation [25] increase permeability across membrane [26, 27] and to change properties of proteins [28]. The cryoprotective property of DMSO was discovered more than 50yrs ago by Lovelock and Bishop [29] and concentrations up to 40% are used in cryopreservation of wide variety of cells [30, 31]. The structure of the model cell membranes (phospholipids bilayers) have been investigated by many experimental studies [32-39]. using X-ray diffraction and differential scanning calorimetry methods. The equilibrium phase changes and kinetics of dipalmitoylphosphatidylcholine (DPPC) with DMSO was investigated by Tristram-Nagle et al. [33] and they attributed the changes in phase behavior to the dehydrating effect caused by DMSO. Yu et al. [34-36] performed X-ray diffraction studies on bilayers with DMSO and found that the thickness of the bilayer decreases and the area per headgroup increases. Kiselev et al. [38]used X-ray diffraction and calorimetry to investigate the influence of DMSO on DPPC bilayers and proposed that DMSO molecules do not penetrate the polar headgroup region or its vicinity. Shashkov et al. (1999) used infrared spectroscopy in addition to x-ray diffraction and calorimetry to investigate the interactions of DMSO and water with bilayer surface and found that the resulting dehydration of the lipid bilayer is caused by the strong interaction between DMSO and water. Chang et al. [73] used calorimetry to study the

effect of DMSO on lipid bilayers and found that the presence of DMSO affects the solvation of the lipid bilayer. Yamashita et al. [115] studied the stability of bilayers in the presence of DMSO at low concentrations and found that the transition temperature from a gel to a liquid crystalline phase increases with increasing DMSO concentration. Although all the experimental studies helped us to study the effect of DMSO on lipid bilayers none of them could actually reveal the intriguing molecular details involved. So, atomistic simulations came into play to study the detailed molecular mechanisms involved in the interactions of DMSO with lipid bilayers.

Recent advances in computational resources have permitted large scale molecular dynamic simulations for studying the interactions of different chemicals on lipid bilayers at molecular level. With computer simulations we can analyze biomembrane properties from atomistic perspective with a degree of detail that is hard to reach by other techniques. The excellent agreement of the results obtained with various molecular dynamics (MD) studies [40, 41] on simple model membranes with experiments has raised the confidence in applying the atomistic simulations to even more complex systems. Although numerous MD simulations have been done to study the interaction of various small molecules on lipid bilayers [27, 41-53], only few computational studies of DMSO have appeared in literature. Paci and Marchi [52] was one of the early studies to study the permeability of glycerolipid bilayer to a polar DMSO molecule. To get more detailed information of DMSO/phospholipid, Smondyrev and Berkowitz [49] studied the properties of lipid bilayers in presence of pure DMSO for time scale of 2ns. They have concluded that there is no larger penetration of DMSO molecules into the membrane and there is no change in the area per lipid. In contrary, Sum and de Pablo [51] showed that DMSO increases the area per lipid and it penetrates much deeper into the bilayer than water. They studied the effect of different concentrations of DMSO at different temperatures, on the structure

of the phospholipid bilayer for a time scale of 10 ns. Although, these MD simulations have shed considerable light on the interactions between DMSO and lipid bilayers, the time scale which was <10ns is not sufficient for the system to get equilibrated. Recent simulations by Moldovan et al [27] and Gurtovenko et al [47] showed that higher concentrations of DMSO leads to pore formation in the bilayer even without the presence of any external forces. Gurtovenko et al studied the effect of different concentrations of DMSO ranging from 0% to 100% on dipalmitoylphosphatidylcholine (DPPC) for a time scale of 30ns. This study showed that at low concentrations of DMSO(<10mol%), DMSO induced membrane expansion which leads to decrease in membrane thickness and concentration of 10mol%-20mol% leads to pore formation and further more increase in concentration leads to disintegration of membrane. We present here the results of constant pressure simulations of Dimyristoylphosphatidylcholine (DMPC) lipid bilayer with low concentrations of DMSO for a time scale of 100ns. Our goal is to compare the structures of DMPC bilayer in presence of low concentrations of DMSO.

3.2 Simulation Model and Methodology

Molecular dynamic simulations were performed on DMPC lipid systems consisting of 96 lipid molecules (48 lipids in each leaflet) in the presence of 3% DMSO (5422 water molecules and 163 DMSO molecules) and 6% DMSO (5422 water molecules and 326 DMSO molecules) solution. Initial arrangement of the simulation system is shown in Fig. 3.1. The MD simulations were performed using the GROMACS 3.3 molecular dynamics package[58]. Isothermal-Isobaric (N,p,T) thermodynamic ensemble is used in which temperature is maintained constant by weakly coupling lipid molecules and water molecules to a temperature bath using Berendsen thermostat [112, 113] with a coupling time constant of 0.1 ps and pressure is maintained at 1 atm using the semi-isotropic pressure coupling to a Berendsen barostat [63] with a time constant of 1.0 ps. The

force field parameters for both bonded and non-bonded interactions were taken from Berger et al.[93]. Periodic boundary conditions were applied along the three space dimensions. The height of the simulation box (z direction) and the cross sectional area (xy-plane) were allowed to vary independently of each other, thereby allowing the area of the bilayers and the distance between the interfaces to fluctuate independently. All bond lengths were constrained to their equilibrium values by the LINCS algorithm [63]. The nonbonded Lennard-Jones interactions were cut-off at a distance of 1.0 nm and the simulation time step was set to 2 fs. Long-range electrostatics were updated every 10 time steps and handled by particle-mesh Ewald (PME) algorithm [116]. An energy minimization procedure based on the steepest descent algorithm was initially applied to the initial structure prior to the actual MD run. The atomic coordinates were saved every 2ps for analysis and total simulation time was 100 ns.

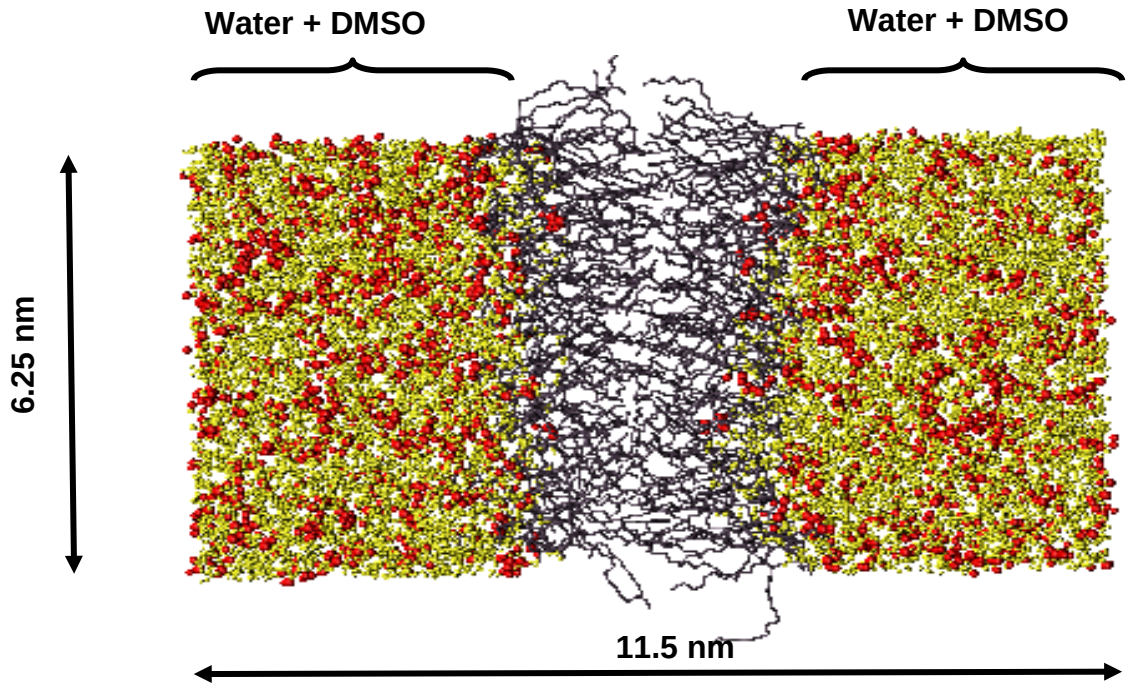

Figure 3-1: Snapshot of the simulation system at 1ns showing the lipid bilayer with water and DMSO molecules (DMSO molecules are shown by van der Waals (vdW) spheres) on either side of the bilayer.

Further details of the simulation can be found in Moldovan et al [27]. Various structural and ordering parameters characterizing the DMPC lipid bilayer exposed to various percentages of DMSO solution were evaluated periodically during the simulation.

3.3 Results and Discussion

Various structural and ordering parameters characterizing the DMPC lipid bilayer interacting with 6 mol % DMSO-water mixture and 3 mol % DMSO-water mixture were investigated. Simulations were analyzed after a running time of 100ns. Fig. 3-2 illustrates the structural changes of DMPC lipid bilayer exposed to water and DMSO solution. It is evident from the snapshots that, there is no penetration of either water or DMSO molecules into the DMPC lipid membrane for a simulation time of 100ns. The various structural and ordering parameters that were analyzed included, i) Area per lipid ii) the mass density profiles across the bilayer of various molecules; iii) various radial distribution functions; iv) the order parameter of the water molecules and v) Deuterium order parameters.

The average area per lipid molecule is one of the most fundamental characteristic of lipid bilayers and it is often monitored in simulations to assess whether or not the system has reached the equilibrium during the subsequent MD run. It is defined by the x- and y- dimension of the simulation system over the number of lipids per layer, i.e., 48 in our case. In general, area per lipid is strongly affected by the presence of various chemicals. Fig. 3-3 shows the time variation of area per lipid for 3% and 6% DMPC-DMSO systems for 100 ns: for reference, area per lipid in pure water is also given. The simulation results show that after an initial transient regime of about 20 ns, the approximate time for the system to attain the equilibrium state, the area per lipid reaches steady values in both systems. The corresponding average values are $\langle A_{3\%DMSO} \rangle = 0.777$ nm^2 and $\langle A_{6\%DMSO} \rangle = 0.824$ nm^2 for 3% and 6% DMPC-DMSO systems respectively.

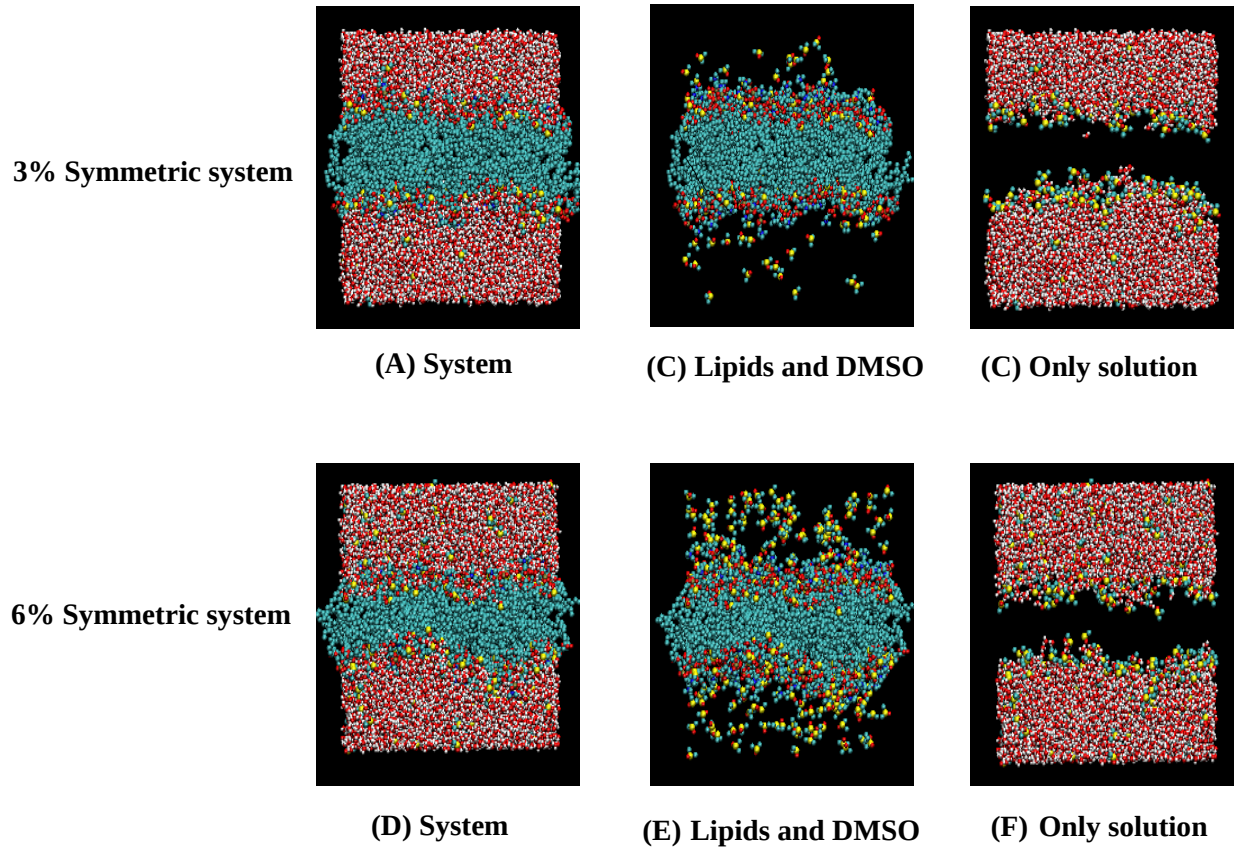

Figure 3-2: Snapshots taken at t = 100ns of the DMPC bilayer in 3mol% DMSO (A,B and C) in 6mol% DMSO (D, E and F). For clarity side views of: whole system (A) and (D); lipids and DMSO (B) and (E); and solution only (C) and (F) are shown.

There is an increase of area per lipid by 18% for 3% DMSO system and 26% for 6% DMSO system. The increase in area per lipid also increases the permeability of the membrane. These results are consistent with the other studies which showed that increase in percentage of DMSO increases the area per lipid [51]. The increase in area is compensated by decrease in thickness of the bilayer which will be further discussed afterwards.

Additional information about the structure of the bilayer in the z-direction can be obtained by analyzing the mass density profiles for lipids, various atomic groups or specific molecules. Fig. 3-4 and Fig. 3-5 depict the mass density profiles of DMPC systems across the bilayers in 3% DMSO and in the presence of 6% DMSO; for reference and comparison the corresponding mass density profiles for pure water system are also given. The lipid mass density

profile gives the distribution of the position of the atoms comprising the lipids along the axis normal to the membrane. The mass density profiles are determined by dividing the simulation

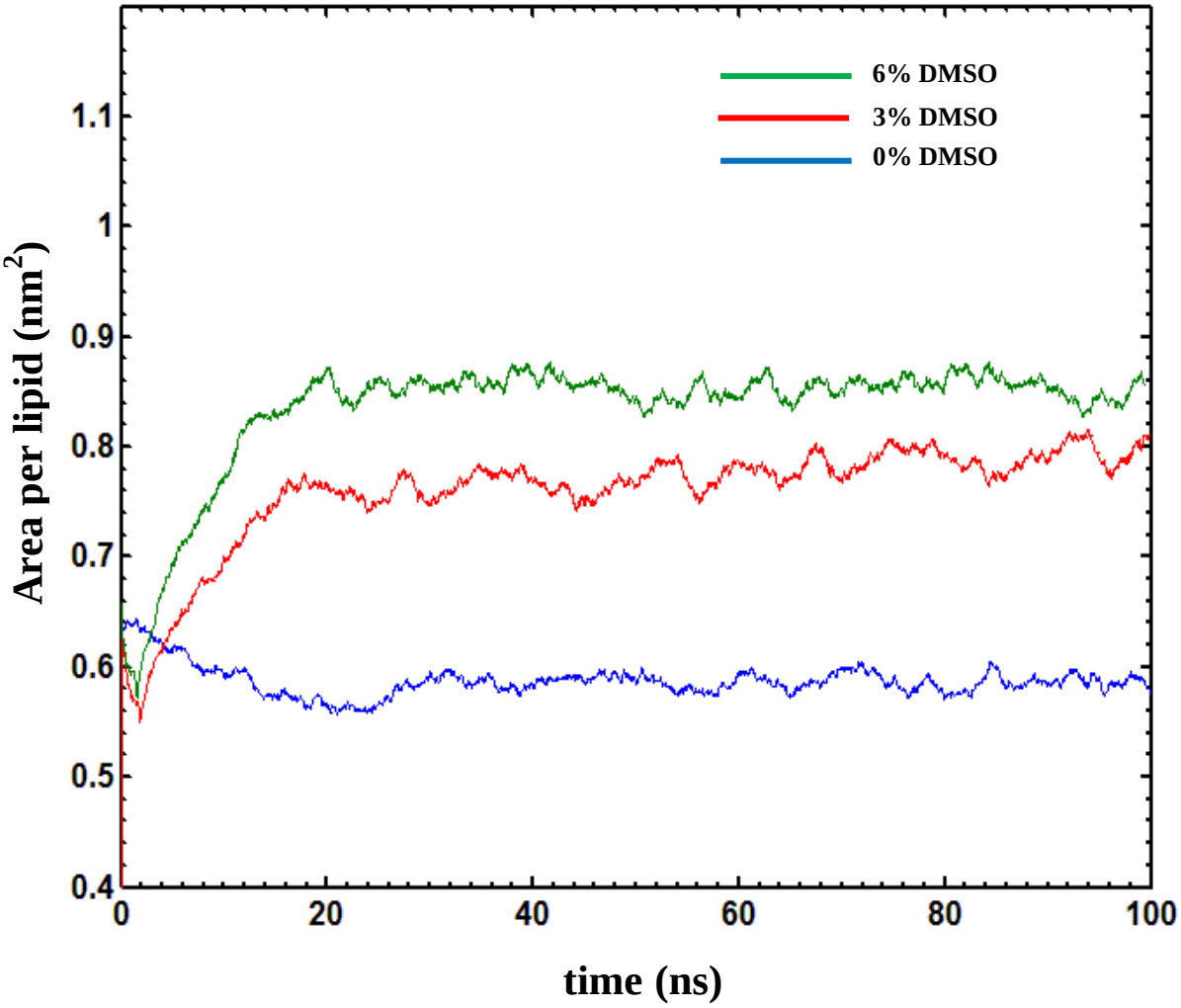

Figure 3-3: Time dependence of the area per lipid for 3% and 6% DMSO system for reference and comparison area per lipd in pure water (or 0 mol % of DMSO) is also included.

box along the direction normal to the membrane into a number of thin slices of equal thickness and subsequently, accounting for type and the total number of atoms located in each slice. This data is then time averaged over a large number of snapshots evenly distributed over the production simulated time interval. The overall DMPC lipid, water and DMSO density profiles

in both 3% and 6% systems shown in Figs. 3 (a) and (b) suggest the presence of three distinct regions, corresponding the aqueous phase, the interface consisting of the lipid head groups and the interior of the lipid bilayer. The reference plane (z=0) is the point of low density, that is the region where the lipid tails meet. By comparing the mass density profiles and the locations of the corresponding three regions one can see that indeed, as demonstrated previously, the presence of DMSO leads to a decrease of the effective thickness of the systems. The actual thickness decrease can be inferred by the difference in distance between the two peaks corresponding to the average position of the lipid head-groups located in the two leaflets. The presence of DMSO leads to a decrease in the average separation between the lipid head-groups by 1.2 nm and 1.6 nm for 3% and 6% DMSO systems respectively. This comparison correlates quite closely with the previously estimated bilayer thicknesses; One can estimate the width of the interface region by using the water density profiles, i.e., the distance over which the water density rises from 10% to 90% of the bulk value.

The motion of the lipid molecules in perpendicular direction to the membrane leads to a rough membrane surface which in time is averaged to a smoothly decaying density profile. The interface width is 1.2 nm and it shows that at fixed temperature the presence DMSO doesn't have any effect on the interface width.

One can gain additional insight into the effect of DMSO on structural changes of the bilayer systems by monitoring Figure 3-5 which shows the mass density profiles along z direction of the two charged groups in the lipid head-groups, specifically the phosphate (P) and the choline (N) groups. These clearly show that DMSO penetrates relatively deep into the membrane and has the tendency to accumulate below the water-bilayer interface and below head-group regions. In fact, as shown in Figures 3-5, the DMSO local density peak seems to be

located roughly close to the average location of the glycerol group of the DMPC lipid. The reduction in the density peaks can be rationalized by realizing that on average the orientation of the vector joining the phosphorous and nitrogen atoms come closer to an in-plane direction (i.e. pointing away from the bilayer normal).

Inorder to gain additional insight into the equilibrated structure of the lipid bilayer we have analyzed the spatial distribution of the various groups/molecules in the system through various radial distribution functions (RDF such as the mutual RDFs between lipid head groups (phosphorous (P-P) and nitrogen (N-N)) or the cross distributions between the head-group atoms and the oxygen atoms of the DMSO (P-O, N-O or C-O). The radial distribution function *g(r)* is often employed to identify close range ordering of neighboring atoms. In this regard, the radial distribution function, *g(r),* is defined as,

$$g(r)=N(r)/4\pi r^2\rho dr,$$

where, N(r) is the number of atoms in spherical shell at distance r and thickness dr from a reference atom, and ρ is the number density taken as the ratio of atoms to the volume of computing box. Thus g(r) measures how atoms organize themselves around each other. The radial distribution function, shown in Figure 3-6, shows g(r) is zero for short distances(less than the atomic diameter) and is due to the strong repulsive forces. At long distances, g(r), tends to one, indicating that there is no long-range order. Figure 3-6 shows the radial distribution for the lipid head groups (P-P and N-N) at different DMSO concentrations. We observed an appearance of a distinct peak in the presence of DMSO. This indicates that the repulsion between the choline groups is reduced, which can also lead to an increase in the interaction between DMPC molecules in the presence of DMSO.

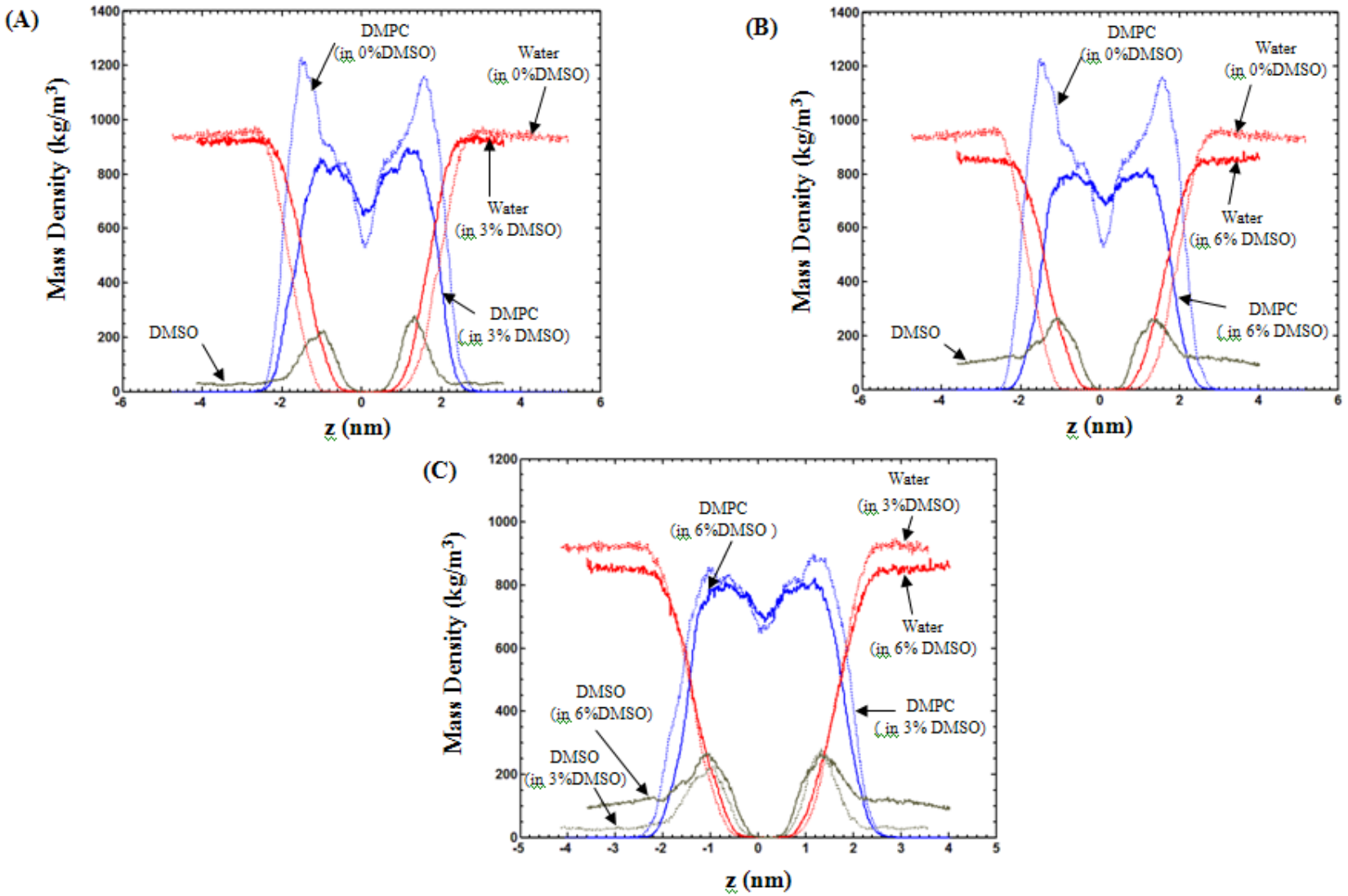

Figure 3-4: Mass density profiles of lipid and water in the presence and absence of DMSO at 100ns (A) 3% DMSO system (B) 6% DMSO system. The mass density profile of DMSO is also shown in both the figures. (C) shows the comparison between 3% and 6%DMSO.

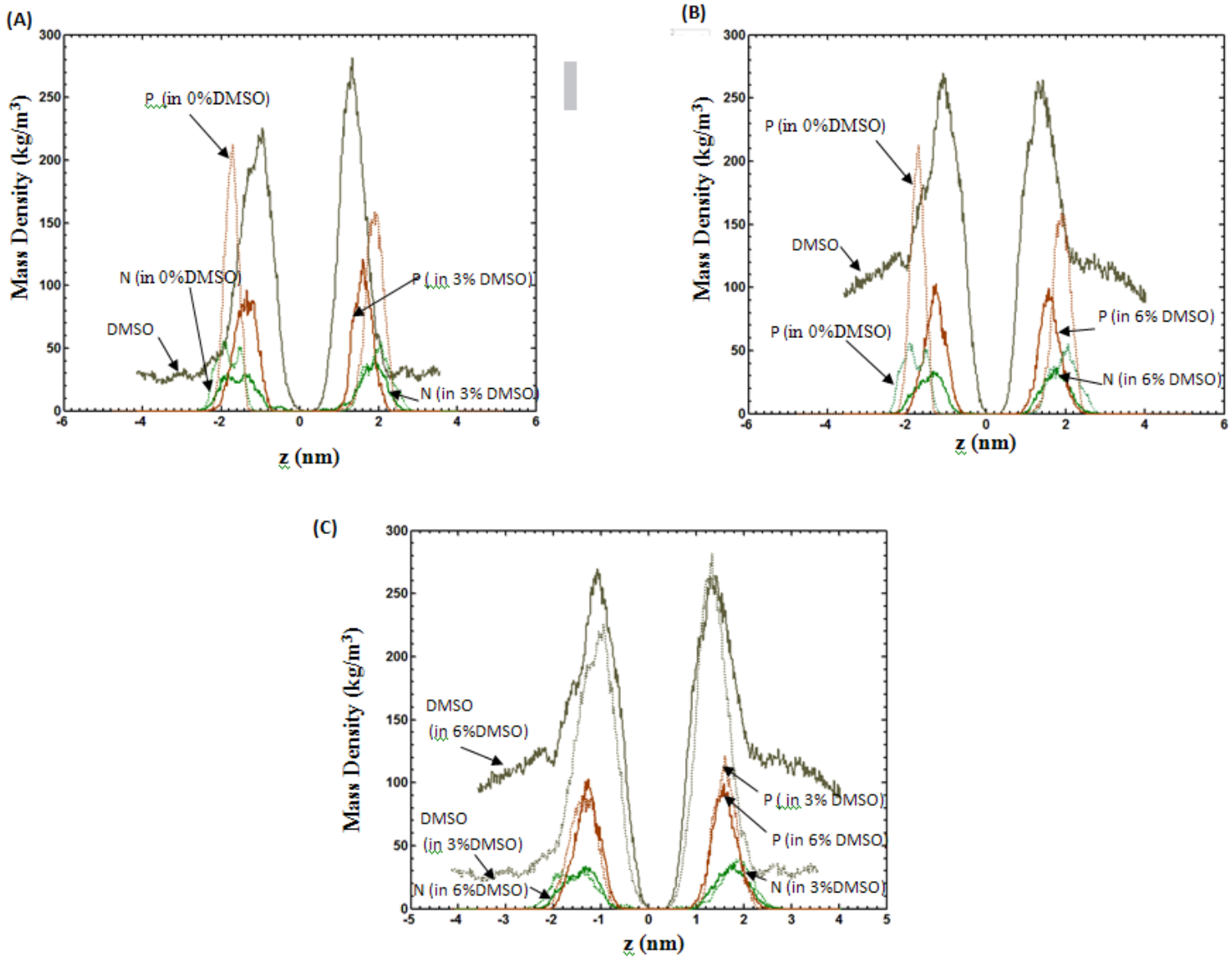

Figure 3-5: Mass density profiles of nitrogen (N) and phosphorous (P) in the presence and absence of DMSO at 100 ns (A) 3% DMSO system (B) 6% DMSO system. The mass density profile of DMSO is also shown in both the figures. The comparison between 3% and 6%DMSO system is shown in figure (C).

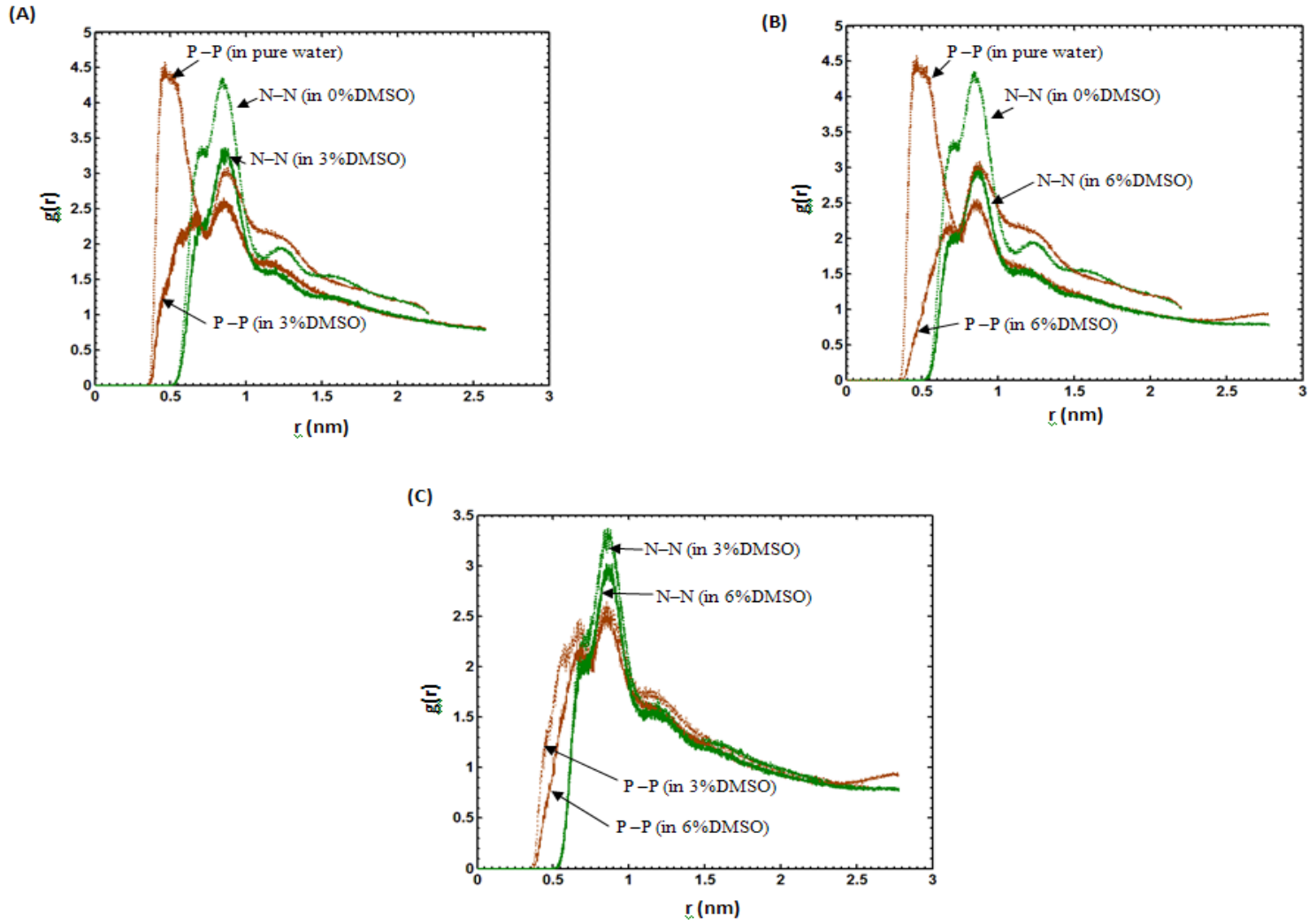

Figure 3-6: Radial distribution functions (RDF) between nitrogen (N-N) and phosphorous (P-P) atoms present in the head-group of the lipids in the presence and absence of (A) 3%DMSO (B) 6% DMSO. The mass density profile of DMSO is also shown in both the figures. The mass density profile of DMSO is also shown in both the figures. The comparison between 3% and 6%DMSO system is shown in figure (C).

In addition to the mass density profiles, another commonly measured quantity that gives valuable information regarding the structure features of the hydrocarbon tails is the deuterium order parameter, S_{CD}. This quantity is accessible by deuterium nuclear magnetic resonance spectroscopy (NMR) measurements and allows a direct comparison between experiments and simulations. Experimentally, deuterium order parameters, S_{CD}, can be obtained from the residual quadrupole splitting in the deuterium NMR spectrum of samples deuterated at different positions. The deuterium order parameter, S_{CD}, typically ranges from 0 to 0.5. The value of 0.5 is associated with an all trans conformation state and a value of 0 is associated with the isotropically disordered state. The deuterium order parameter, S_{CD}, is related to the components of the order parameter tensor $S_{\alpha\beta}$ defined as:

$$S_{\alpha\beta} = \frac{1}{2}\langle 3\cos\theta_\alpha \cos\theta_\beta - \delta_{\alpha\beta}\rangle \tag{3.2}$$

where α, β = x, y, z and θ_α is the angle between the molecular α-axis and the bilayer normal (z-axis). The brackets "< >" denote a time average over an ensemble of configurations. The molecular axes must be defined separately for each segment of an acyl chain. Usually for the C_n methylene group the $C_{n-1} - C_{n+1}$ direction is taken as z, and the $C_{n-1} - C_n - C_{n+1}$ plane is the *yz* plane. Since the bilayer is symmetric with respect to the rotation around z-axis (perpendicular to the bilayer), we have $S_{xx} = S_{yy}$ and $S_{xx} + S_{yy} + S_{zz} = 0$. Moreover, the relevant order parameter is the diagonal element, S_{zz} ,which is related to the deuterium order parameter, S_{CD}, defined as:

$$S_{CD} = -\frac{2}{3}S_{xx} - \frac{1}{3}S_{yy} \tag{3.3}$$

Given the system symmetry we can simply write $S_{CD} = 1/2S_{zz}$. From the simulations the order parameter is calculated separately for all carbon atoms along the acyl chain.

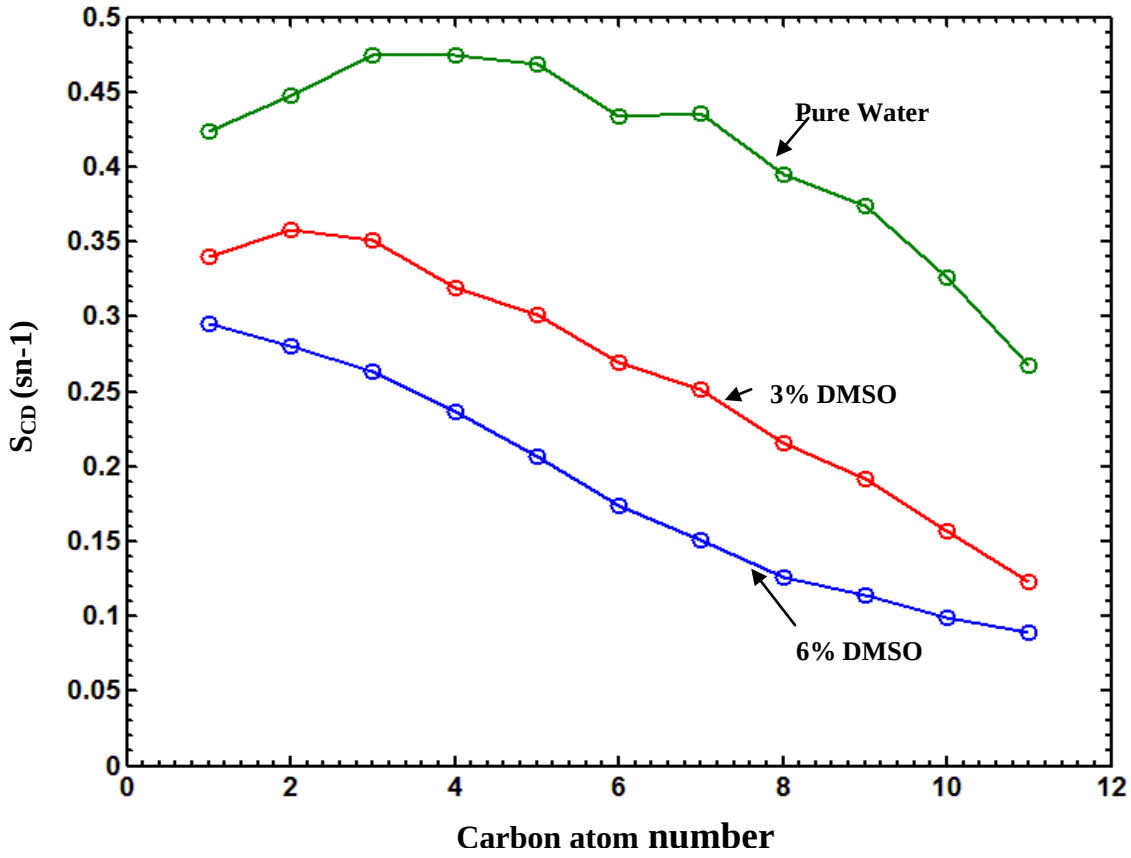

Figure 3-7: Deuterium order parameters, SCD, for sn-1 chain in DMPC bilayer at 100ns.

The deuterium order parameter for DMPC lipid tails in different percentages of DMSO are shown in Fig. 3-7. The simulation results clearly show that the increase in DMSO decreases the ordering of along the lipid tails which are in agreement with previous simulations. The disorder in lipid tails is related to increase in area per lipid, the more loosely is the alkyl tails packing the more disordered they are. Indeed, as discussed in the previous sections, in the presence of 3mol% and 6mol% of DMSO, the area per lipid in the DMPC bilayer increases by ~18% and 26%. This substantial increase of the area per lipid is expected to substantially influence the packing and ordering in both head and tails regions and possibly leading to an increase of disorder along the chains.

Important information regarding the water ordering in the vicinity of the bilayer-water

interface (hydration layer) can be obtained from studying the mean cosine value, $\langle cos\theta \rangle$, of the angle between the water dipolar moment $\bar{\mu}$ and the bilayer normal unit vector $\bar{n}$. That is,

$$\langle cos\theta(z) \rangle = \frac{1}{\bar{\mu}(z)} \langle \bar{\mu}(z).\bar{n} \rangle \qquad (3.4)$$

where z is the z-coordinate of the centre of mass of the water molecules. The mean cosine value is obtained by averaging, in the equilibrium regime, over dipolar orientations of all water molecules present in the system and over a large number of equilibrium states. Fig. 3-8 shows the results from our MD simulations for the ordering of water in the vicinity of a DMPC lipid bilayer system with different percentages of DMSO. When generating Fig. 3-8 the normal unit vector, $\bar{n}$ parallel to the z-axis was considered to have the same orientation for the solvent on both sides of the bilayer. Consequently, by symmetry, the cosine average has opposite sign in the two regions. $cos\theta = 0$ indicates that there is no permeation of water molecules inside the membrane. Distance between the peaks gives the thickness of the bilayer. From the Fig. 3-8, one can clearly see that in the presence of DMSO the ordering of the water molecules in the hydration layer decreases (as evidenced by the decrease in the peak heights in Fig. 3-8. In addition, the presence of DMSO also leads to the decrease of the separation distance between the two hydration layers present on both sides of the membrane. Assuming that the thickness of the hydration layers does not change substantially by the addition of DMSO, the change in the separation of the hydration layers can be attributed entirely to the change of the bilayer thickness. The large increase in the area per lipid of the DMPC lipid bilayer might be the primary reason for the large variation in the bilayer thickness of the DMPC bilayer (can be notified by the huge difference between the two peaks on either side of the center of the bilayer). The increase in area per lipid may possibly lead to an increase in the membrane permeability. This increase in the

membrane permeability might be a primary reason for the ability to successfully cryopreserve biological systems at a higher cooling rate in the presence of chemicals (like DMSO) than in their absence [30, 31].

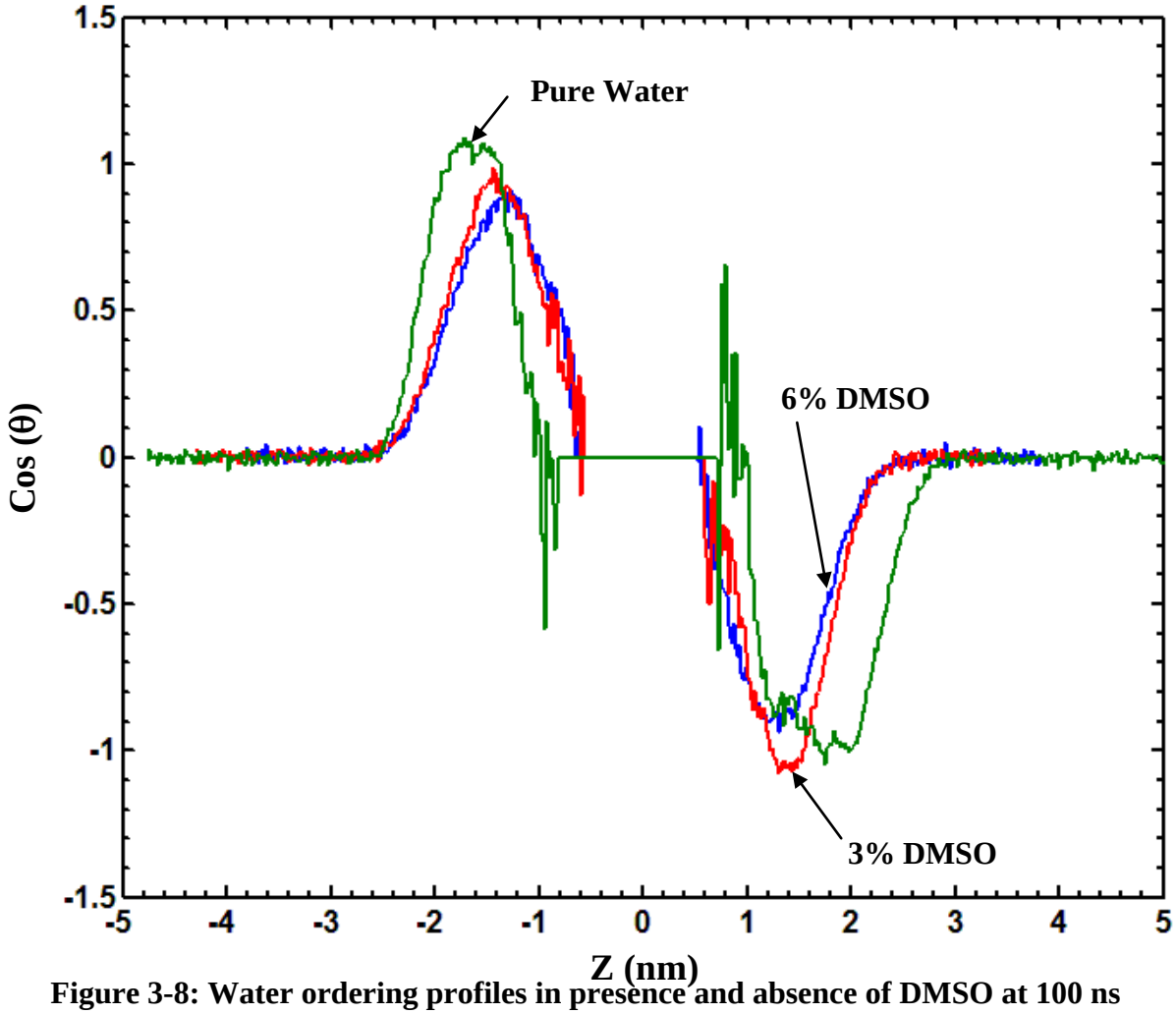

Figure 3-8: Water ordering profiles in presence and absence of DMSO at 100 ns

3.4 Conclusions:

The aim of this study was to develop an understanding of the effect of low and moderate concentrations of DMSO on lipid bilayers membranes exposed symmetrically to thw water-DMSO solution. The simulations show that: i) the DMSO molecules have the tendency to accumulate in a layer below the membrane-water interface (near the carboxyl group); ii) with

increase in DMSO concentration the ordering of the lipid head-groups in DMPC is lowered; and iii) there is an increase in the area of per lipid in 3% DMSO system by and in 6%DMSO system when compared with the values obtained in the absence of DMSO. Our simulation results also indicate that the area per lipid molecule and the ordering of the alkyl tails are strongly anti-correlated and increase in the area per molecule is accompanied by a decrease in the tails order parameter.

4 INVESTIGATION OF STRUCTURAL CHANGES OF LIPID BILAYERS INDUCED BY DIMETHYLSULFOXIDE: ASYMMETRIC BILAYER SYSTEM

4.1 Introduction

In a typical cryopreservation protocol, the system to be preserved is first equilibrated with chemicals known as cryoprotective agents (CPAs). The study of the effects of CPAs on membranes is very important in many biological and medical applications. For example during freezing preservation, chemicals denoted as cryoprotective agents (CPAs) have long been utilized to minimize freezing injury [11]. Commonly used CPAs include glycerol, dimethylsulfoxide and methanol. CPAs have been shown to alleviate cell damage from either the solute effects or the formation of intracellular ice during the subsequent freezing process. The transfer of cryoprotective agents (CPAs) through membranes, play a major part in cryopreservation [3]. To develop mechanistic and rational understanding of cryopreservation processes it is important to study the interactions of CPAs with cell membranes. Lipid molecules, the main components of the cell membranes, are either polar or charged and they interact strongly with each other, with the polar water or non-water environment, with counter ions [117] and proteins [35], or with DNA [92]. These interactions play a major role on the structural and dynamical characteristics of the membranes. Understanding such interactions at molecular perspective through atomistic simulation techniques is of great biological and medical interest. One of the most widely used cryoprotective chemical is Dimethylsulfoxide (DMSO) and its aqueous solutions. DMSO ($(CH_3)_2SO$) solubilizes a wide variety of compounds due to the presence of a polar S = O group and two hydrophobic CH_3 groups. Aqueous DMSO induces cell fusion [24], cell differentiation [25] and increases membrane permeability [118]. It exhibits

significant pharmacological activity, anti-inflammation effect, analgesic effect, antivirial, antibacterial activity and radioprotection abilities [109]. In most cases DMSO penetrates cell membranes in order to exert its protective ability, this has led to numerous studies and hypothesis about its properties and interactions with biological membranes.

Molecular dynamics methods have been used extensively used to model DMSO/water mixtures [119-123]. Numerous MD simulations have been done to study the interaction of various symmetric concentration of DMSO molecules on lipid bilayers [27, 41-53], but in reality when we add CPA to cell suspension the concentration outside the cell will be more than the concentration inside the cell. So the cell membrane is exposed to asymmetric concentration of CPA and therefore the influence of CPA on the inner leaflet and outer leaflets of the membrane can differ considerably. Only few simulations appear in literature studying the effect of asymmetric composition on lipid bilayers [124-126]. Gurtovenko [124] studied the effect of asymmetric composition of monovalent salt on lipid bilayers and found that a slight asymmetry in the charge distribution between the two bilayer leaflets results in a nonzero potential difference of about 85 mV between the two water phases. Lee et al [126] studied the effect of asymmetric ionic concentration across the lipid bilayer and found that there is a large potential difference of -70mV across the two water chambers. We present here the results of constant pressure simulations of Zwitterionic Dimyristoylphosphatidylcholine (DMPC) lipid bilayer with asymmetric composition of DMSO across the bilayers. Our goal is to study the structural changes induced due to asymmetric concentrations DMSO on DMPC bilayer.

4.2 Simulation Methodology

In the present study, zwitterionic Dimyristoylphosphatidylcholine (DMPC) lipid was used as a cell membrane model. The DMPC lipid within a united atom representation consists of

46 interaction sites (Figure 4-1). Force-field parameters for the DMPC lipids were taken from the united atom force field of Berger [93]. This force field was previously validated [27, 53] and was shown to reproduce experimentally observed values of the area per lipid.

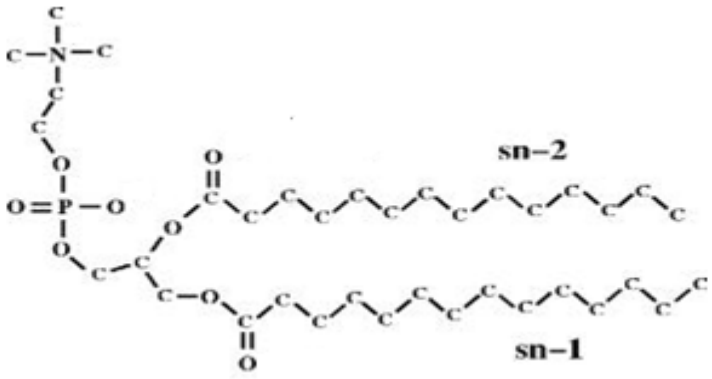

Figure 4-1: Chemical structure of a zwitterionic dimyristoylphosphatidylcholine (DMPC) lipid.

The asymmetric simulation model employed in the present study is depicted in Figure 4-2. As indicated in Fig. 4-2, the central region, between the two bilayers had pure water while the outside two regions consisted of water/DMSO mixture. Due to the periodic boundary conditions considered in the MD simulations the outside two regions containing the DMSO solution constituted a single contiguous volume. Such a model setup was recently used for modeling the salt gradient across a phosphatidylcholine bilayer [124]. The MD simulations were performed using GROMACS molecular dynamics package. The height of the simulation box (z direction) and the cross sectional area (xy-plane) was allowed to vary independently of each other, thereby allowing the area of the bilayers and the distance between the interfaces to fluctuate independently. The force field interactions employed for the simulations are summarized in Moldovan et al [2]. An energy minimization procedure based on the steepest descent algorithm was initially applied to the model prior to the actual MD run. The atomic coordinates were saved every 2ps for analysis and total simulation time was 50 ns. Simulations were done at two

different concentrations of DMSO (3% and 6%) in the outside domain of the simulation box. Various structural and ordering parameters characterizing the DMPC lipid bilayers asymmetrically exposed to water and water/DMSO solution were evaluated periodically during the simulation.

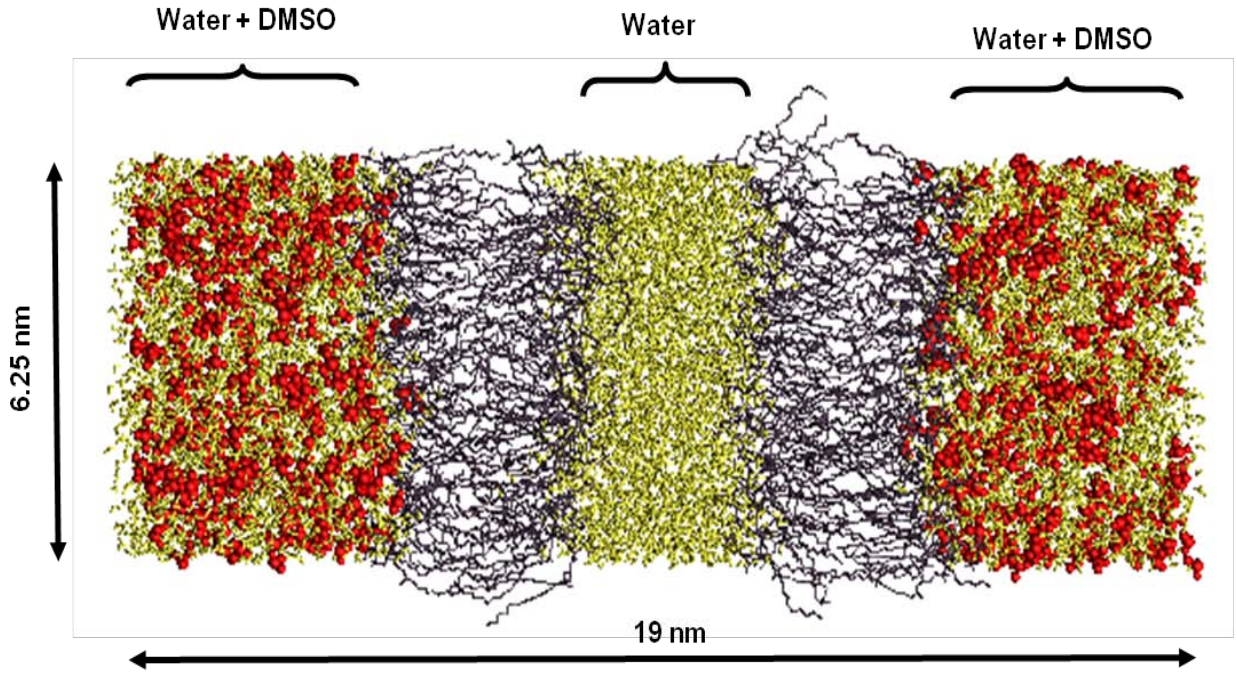

Figure 4-2: Snapshot at 1ns showing the setup of the asymmetric system consisting of: two lipid bilayers, an "inner" domain containing pure water, and the "outer" domain containing water-DMSO solution (DMSO molecules are represented as van der Waals (vdW) spheres).

4.3 Results and Discussion

Figure 4-3 illustrates the structural changes of the DMPC lipid bilayer asymmetrically exposed to water and DMSO solution. As evident from the three sets of side view representation of the lipid bilayer system for two different concentrations there is no penetration of either water or DMSO molecules into the lipid bilayers even after a simulation time of 50ns. However, the lipid leaflets had undergone structural changes due to the presence of solution mixtures. The lipid leaflet exposed to water/DMSO mixture had undergone major structural changes when

compared to the leaflet exposed to pure water. The reason for this might be attributed to the stresses induced by edge active agents. Future sections of the chapter will be focused on the illustration of the structural changes through the study of area per lipid, mass density across the normal, tail order parameter and water ordering profiles.

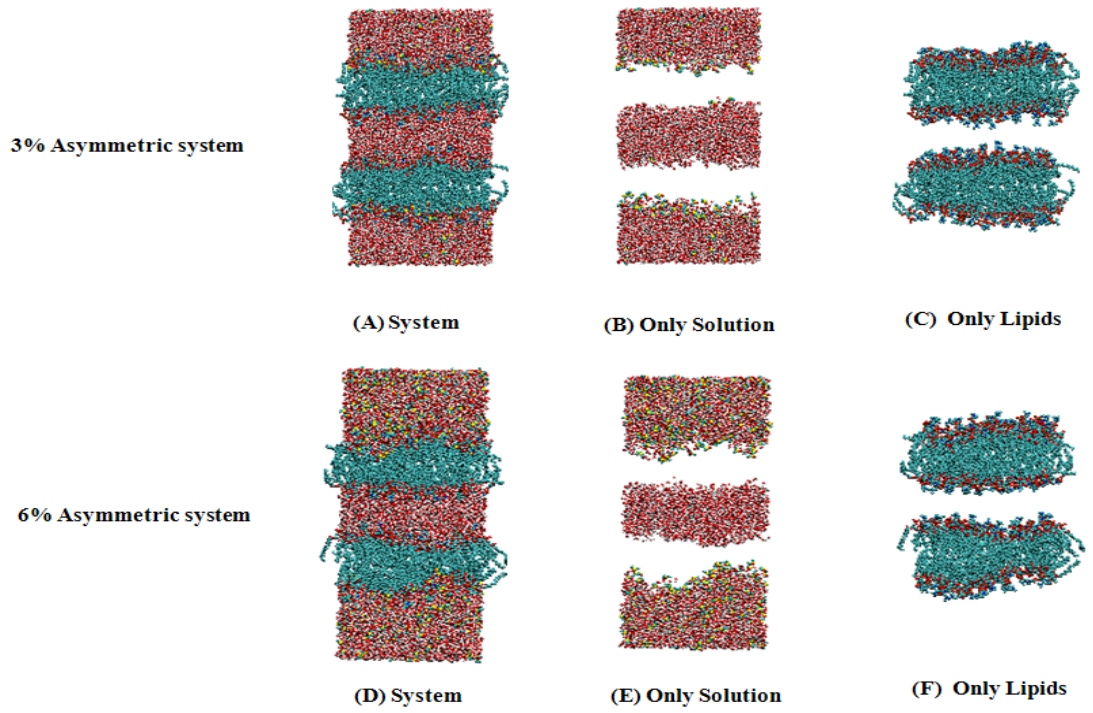

Figure 4-3: Snapshots taken at t=50ns of the two DMPC bilayers exposed asymmetrically to water and water-DMSO solutions of 3mol% DMSO (A, B and C) and 6mol% DMSO (D, E and F) respectively. For clarity side views of: whole system (A) and (D); lipids and DMSO (B) and (E); and solution only (C) and (F) are shown.

Figure 4-4 shows the time dependence of the area per lipid (for a simulation of 50 ns) of the asymmetric systems. For reference and comparison the area per lipid of various symmetric systems is also shown in the figure. As discussed in chapter 3, for a symmetric system, the increase in the concentration of DMSO increased the area per lipid of the system. For example, there was an increase of ~12% in the area per lipid when the concentration of DMSO was increased from 3% to 6%. However, in the case of asymmetric system, as evident from Figure 4-

4, we do not witness any significant change of the membrane. The effect of the increase in concentration of DMSO on the area per lipid had been negated due to the presence of asymmetric boundaries on each individual lipid leaflet of the bilayer. Although the edge active agent (DMSO) induced structural changes in the outer leaflets of the membranes, leading to a considerable change in the area per lipid of the outer leaflet (lipid leaflet exposed to water/DMSO solution) the inner leaflet (lipid leaflet exposed to water solution) remain largely unaffected and maintains the apparent area per lipid in both membranes unchanged.

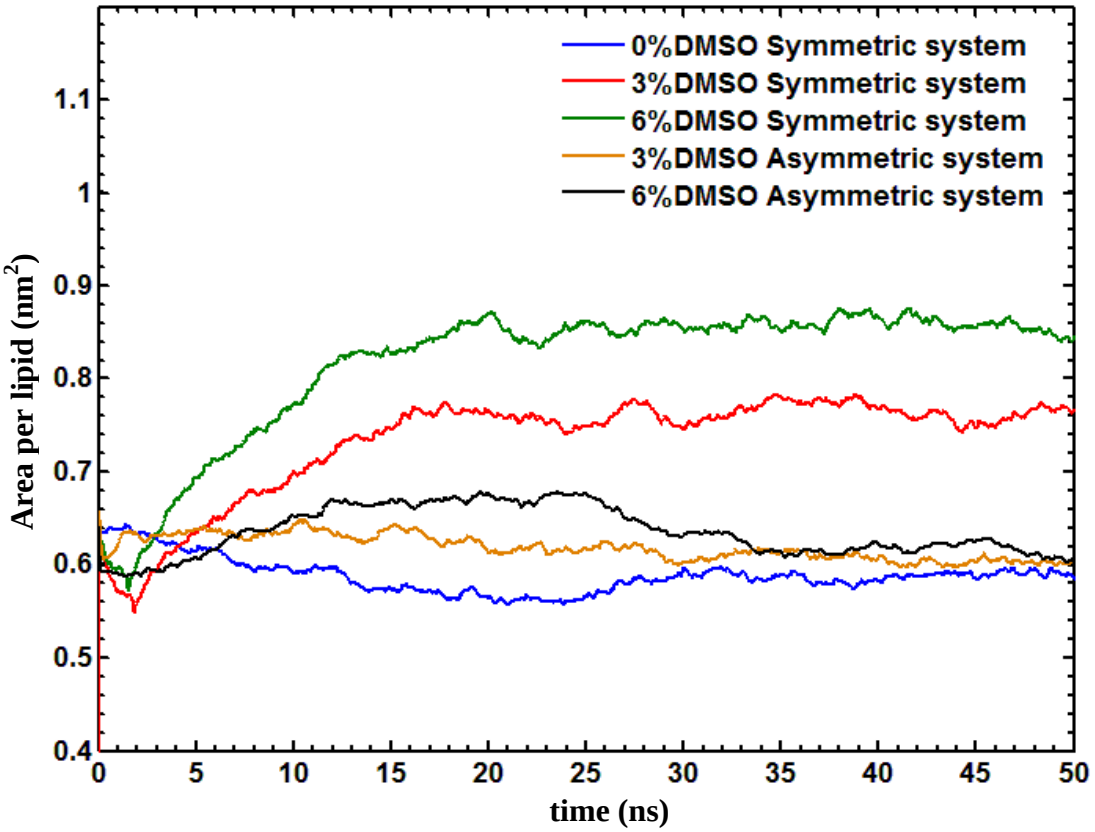

Figure 4-4: Time dependence of area per lipid for 50ns.

Figure 4-5 show the mass density profiles of the lipids, DMSO and water across the z-direction in the presence of 3% DMSO (a) and 6% DMSO (b) for a simulation time of 50 ns. The difference in the adjacent peaks of the lipid density profile gives the thickness of the bilayer

(shown in shaded colors in the Figure). It is evident from the figure that there is a decrease in the thickness of the bilayer with an increase in the concentration of DMSO. The lipid density curve depicted in Figure 4-5 clearly suggests us that there is no changes in the leaflet which is exposed to pure water whereas there is a decrease in height as well as widening of the peaks corresponding to the lipid leaflets exposed to DMSO. This result is consistent with a higher degree of disorder of the lipids forming these leaflets (witnessed from simulations). Associated with the increase of the structural disorder in these leaflets we have a corresponding accumulation of both DMSO and water molecules in the head regions of the two outer leaflets. The decrease in thickness of the bilayer in asymmetric system is less when compared to the values of symmetric system (as shown in Table 4-1), the observed change in membrane thickness is presumably due to the decrease in ordering of the lipid chains. In addition to the mass density profiles, another commonly measured quantity that gives valuable information regarding the structural features of the hydrocarbon tails is the deuterium order parameter, S_{CD}. Figure 4-6 shows the deuterium order parameter for sn-1 in DMPC lipid tails for concentrations of 3% and 6% DMSO in the case of asymmetric system. In the figure inner leaflet represents the leaflet which is exposed to pure water and outer leaflet represents the leaflet which is exposed to water/DMSO solution. It can be observed that the tails in the leaflet which are exposed to DMSO are more disordered than the tails in the leaflet which is exposed to pure water. It can also be inferred that tails exposed to 6% DMSO solution are more disordered than the tails which are exposed to 3% DMSO solution.

Table 4-1: Summary of MD simulations of lipid bilayer systems.

Type	%DMSO	No of Atoms	No of Lipids	No of Water	No of DMSO	<*A*> (nm^2)	Thickness (nm)
Asymmetric system	3%	33231	192	8133	156	0.6 ± 0.01	2.9 ± 0.2
	6%	34479	192	8133	312	0.61 ± 0.03	2.6± 0.3
Symmetric system	0%	20662	96	5422	0	0.59 ± 0.01	3.6 ± 0.12
	3%	21286	96	5422	156	0.777 ± 0.02	2.4 ± 0.37
	6%	21910	96	5422	312	0.824 ± 0.03	2.0 ± 0.21

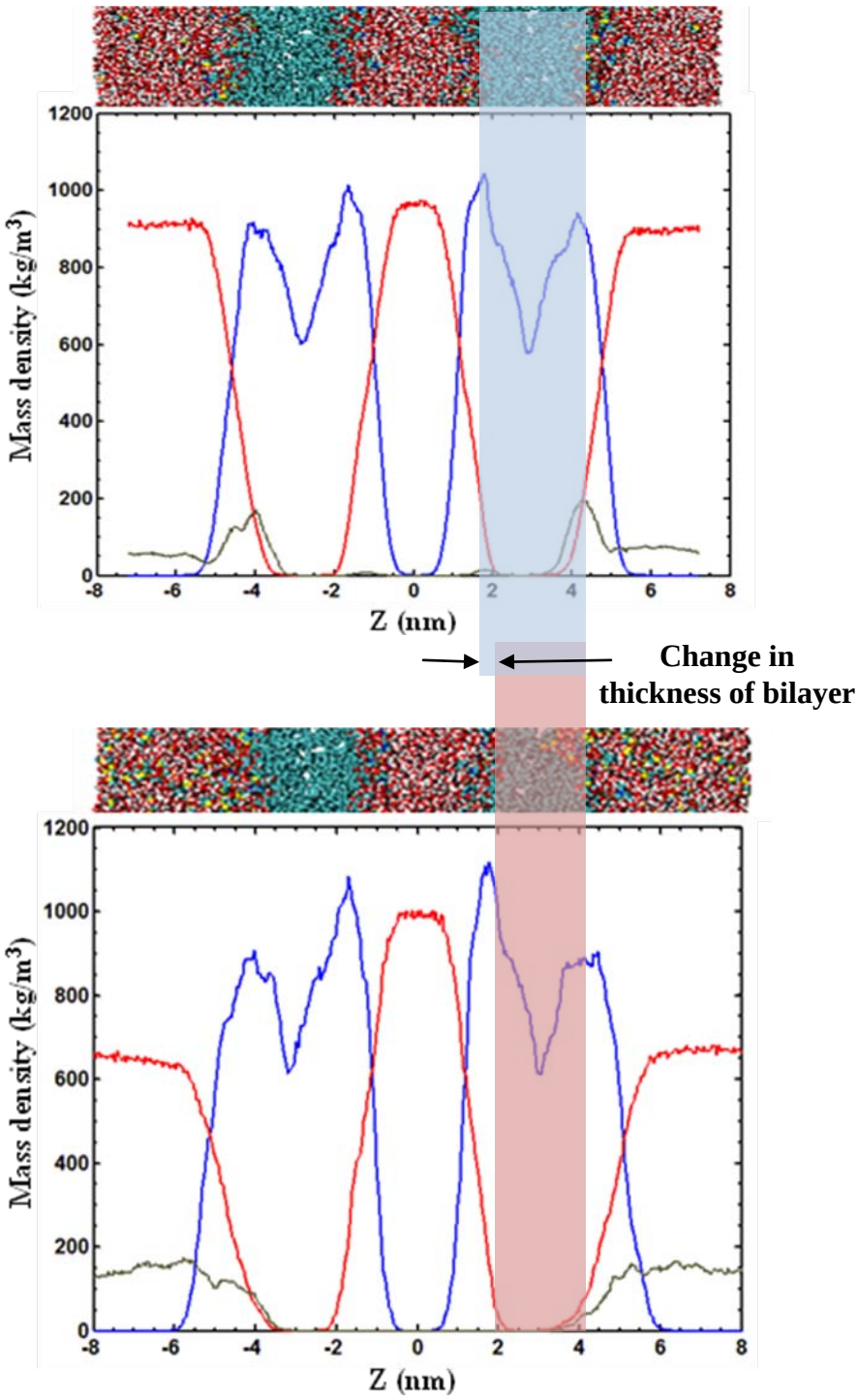

Figure 4-5: Mass density profiles of water (red line), DMSO (green line) and lipids (blue line) across the DMPC. (A) 3% Asymmetric system, (B) 6% Asymmetric system for 50ns.

The simulation results clearly show that the increase in DMSO decreases the ordering of the lipid tails which are in agreement with previous simulations. The disorder in lipid tails is due to the widening of the leaflet exposed to DMSO, the more loosely is the alkyl tails packing the more disordered they are. Indeed, as discussed in the previous sections, in the presence of 3% and 6% of DMSO, the outer leaflet (leaflet exposed to water/DMSO solution) gets widened and the thickness of bilayer decreases by 0.7 nm and 1.0 nm respectively. This widening of the leaflet is expected to substantially influence the packing and ordering in both head and tails regions of the lipid and may possibly lead to an increase of disorder along the chains.

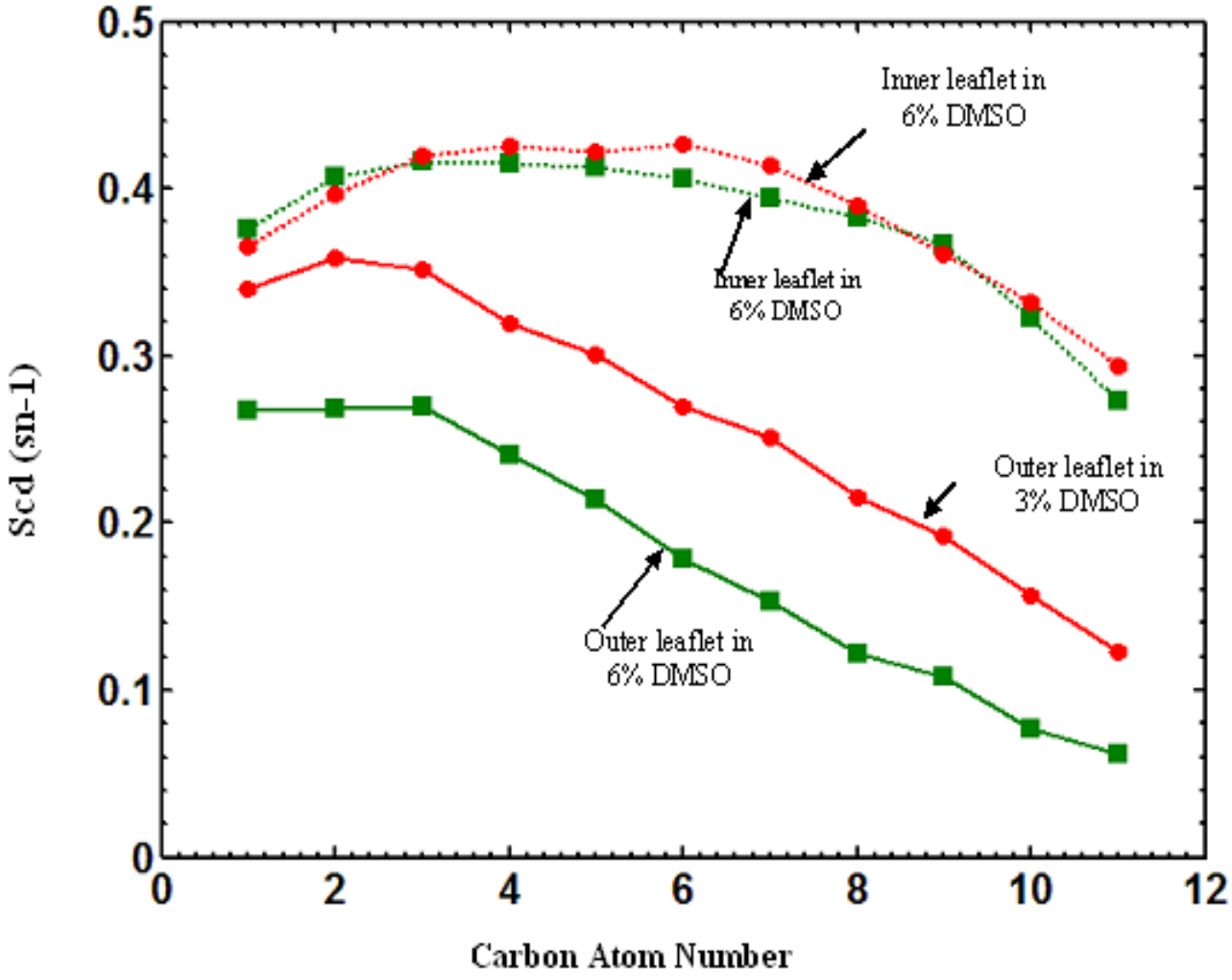

Figure 4-6: Deuterium order parameter for sn-1 after 50ns.

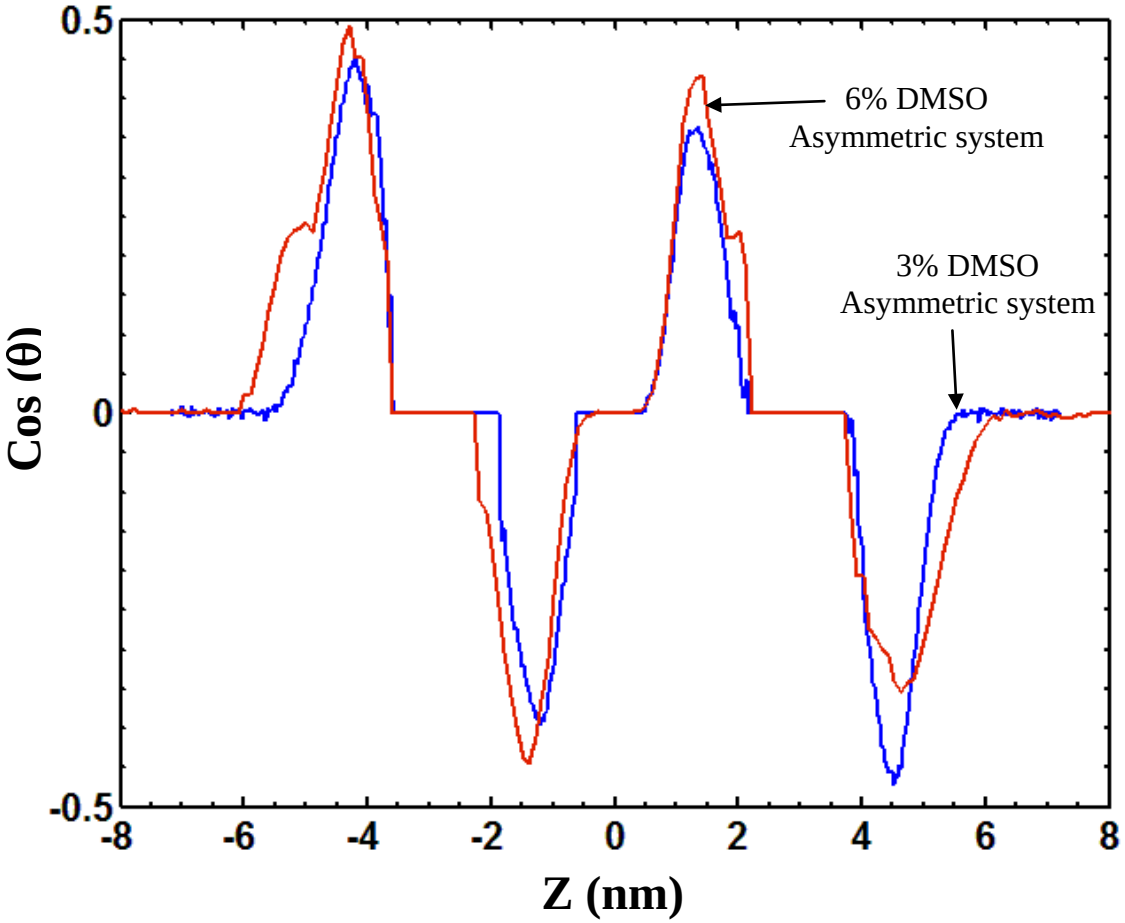

Figure 4-7: Water orientation profiles for 3% DMSO asymmetric system and 6% DMSO asymmetric system

Important information regarding the water ordering in the vicinity of the bilayer-water interface (hydration layer) can be obtained from studying the mean cosine value, $\langle \cos\theta \rangle$, of the angle between the water dipolar moment $\overline{\mu}$ and the bilayer normal unit vector $\overline{n}$ [3]. Figure 4-7 shows the water ordering profiles in the case of asymmetric system with 3% and 6% DMSO for a simulation time of 50 ns. It is evident from the figure that in the presence of DMSO the ordering of the water molecules in the hydration layer decreases (as evidenced by the decrease in the peak heights near the water/DMSO solution). In addition, the presence of DMSO also leads to the decrease of the separation distance between the two hydration layers (as shown by the

shaded colors). Assuming that the thickness of the hydration layers does not change substantially by the addition of DMSO, the change in the separation of the hydration layers can be attributed entirely to the change of the bilayer thickness. The shift in peaks observed between the 3% DMSO and 6% DMSO is another important indication of the major effect of DMSO on the outer leaflets.

4.4 Conclusions

The aim of the present study was to investigate the effect on structural properties of asymmetric exposure to water and water-DMSO solutions of lipid bilayers. We present here the results of constant pressure simulations of Zwitterionic Dimyristoylphosphatidylcholine (DMPC) lipid bilayer with asymmetric composition of DMSO across the bilayers. The simulations were run for over 50 ns, and the structural changes were studied by characterizing: the area per lipid, mass density profiles across the bilayer, tail order parameters and water ordering profiles. The simulations suggested that: i) the structural rearrangement to the leaflet exposed to water/DMSO solution was higher when compared to the leaflet exposed to pure water ii) the DMSO molecules had a tendency to accumulate in a layer below the membrane-water interface (near the carboxyl group); iii) the tails in the leaflets which are exposed to DMSO are more disordered when compared to the tails in the leaflet which is exposed to pure water. iii) the increase in the area per lipid with increase in DMSO concentration was minimal in the case of asymmetric system when compared with that of symmetric system.

5 MOLECULAR DYNAMICS SIMULATIONS OF PORES GROWTH IN LIPID BILAYERS

5.1 Introduction

Biological membranes are sheet-like assemblies of complex mixture of lipids, proteins, and carbohydrates. The most basic property of membrane is that of acting as a barrier between the inside and outside of a cell, depends strongly on the continuity and integrity of the bilayer structure. However, membranes are not impenetrable walls. There is transport of small molecules across the membrane; fusion and cell lysis may cause partial breakdown of the lipid membrane. One important state in which the continuity and integrity of the lipid membrane is lost (at least locally) is due to the formation of ion specific channels and pores. The major difficulty in studying trans-membrane pores experimentally is that they are usually below the theoretical resolution of light microscope**.** So understanding the formation of pore and their stability is of great importance. Recent evolution of realistic atomic level computer simulations have allowed the investigation pores produced by the application of external forces such as mechanical stresses [127] or electric fields [128]. However, very recent simulations by Moldovan et al [27] and Gurtovenko et al [47] showed the formation of pores due to the presence of high concentrations of DMSO in the absence of any external forces. Gurtovenko et al [47] studied the effect of different concentrations of DMSO ranging from 0% to 100% on dipalmitoylphosphatidylcholine (DPPC) for a time scale of 30ns. They have shown that low concentrations of DMSO(<10 mol%) had induced membrane expansion which lead to a decrease in membrane thickness and concentration between 10 mol%-20 mol% lead to pore formation and furthermore increase in concentration lead in the disintegration of membrane. Moldovan et al [27] studied the effect of 11.3 mol% of DMSO on DMPC for a time scale of 100 ns. They have shown the formation of

pores and rationalized the nucleation process in terms of a simplified free energy model that includes the entropy of the pore shape. By estimating the line tensions within the lipid bilayers with and without edge-active agents (DMSO), their simulations were corroborated with the pore growth model. They found out the critical line tension value to be 5.9 *pN*, and showed that DMSO molecules perturb lipid cohesion around the pore edge in DMPC lipid bilayers leading to lowering of the line tension and the corresponding barrier for pore creation. In the present study we report our recent simulation results on the effect of DMSO concentration ranging between 3 mol% - 9 mol% on DMPC lipid bilayer line tension and DMPC lipid bilayer structural stability with respect to pore nucleation.

5.2 Simulation Methodology

The MD simulations were performed with the GROMACS molecular dynamics package. Several sets of MD simulations were carried out on DMPC lipid bilayers immersed in pure water, and DMSO-water solution at four different concentrations. Systems at four DMSO concentrations (3 mol %, 6 mol %, 9 mol%) were thoroughly investigated with the lipid bilayers in fluid phase and in equilibrium at 323K. Further details of the simulation methodology can be found in chapter 3. The line tension, λ, of a linear DMPC bilayer edge, in the presence of varying concentrations of DMSO-water solutions, were calculated from separate simulations using the method developed by Tolpekina et al [129]. Ribbon-like (strip) bilayers as shown in Fig 5-1, consisting of 96 lipids surrounded by water (or by water and DMSO) molecules in the normal (x) and one of the lateral (y) directions, were simulated using periodic boundary conditions in x, y, z directions. The length of the simulation box along the z axis (parallel to the ribbon edge) was fixed, whereas the box dimensions in the x and y directions were scaled jointly. Through this semi-isotropic pressure coupling scheme, a positive line tension is supported along the ribbon edges while

system's volume is allowed to change and equilibrate at 1 atm pressure. The positive line tension, λ, was calculated from the diagonal elements P_{ij} of the pressure tensor according to the relation shown in Eq 5.1, where <…> stands for time averaging. Further simulation details are available elsewhere [27].

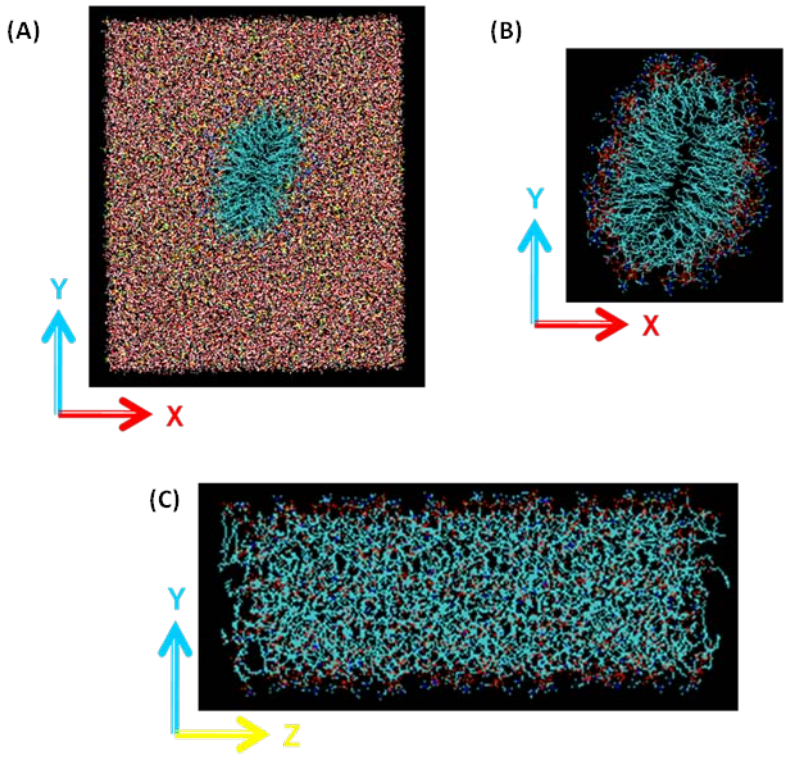

Figure 5-1: Snapshots of the top view and side view of the line tension simulation system. (A) top view of the total system (B) top view of only lipids (C) side view of only lipids

$$\lambda = \left\langle \left(\frac{L_x L_y}{2}\right)\left[\left(\frac{P_{xx}+P_{yy}}{2}\right) - P_{zz}\right]\right\rangle \qquad (5.1)$$

To check the possibility of closing the hydrophilic pores witnessed at higher concentrations of DMSO [27, 47], separate simulation was performed by reducing the concentration of DMSO. The methodology adopted in the present study to reduce the concentration of DMSO was to add water to the 11.3 mol % DMSO system at 20 ns (where hydrophilic pore was clearly seen [27]).

The DMSO concentration was reduced to 3 mol% and simulations were ran for 100 ns. Additional line tension simulations were also performed at reduced concentrations of DMSO (3 mol%, 6 mol%, 9 mol%) for a simulation time of 30 ns.

5.3 Results and Discussion

Moldovan et al 2007 [27] showed that DMSO molecules perturb lipid cohesion around the pore edge in DMPC lipid bilayers leading to the lowering of line tension and the corresponding barrier for pore creation. Based on the extended pore nucleation model that accounts for pore shape entropy [130] the threshold line tension, λ*, for pore formation was calculated based on Eq 5.2,

$$\lambda^{*} = \frac{C k_B T}{b} \tag{5.2}$$

where $b = 2\sqrt{\frac{\langle A \rangle}{\pi}}$ is the average lipid head diameter, <*A*> is the average area per lipid prior to pore formation, k_B is the Boltzmann constant, T is the temperature and C is a numerical parameter of the order of unity. Using the simulated area per lipid, <A> ≈ 0.8 nm ^{2}, the typical lipid head size is $b \approx 1$ nm and the line tension threshold for the stability bound of DMPC lipid bilayer at room temperature (T = 300K) is $\lambda^* \approx 5.9$ *pN*.

Further Evidence of Entropic Driven Pore Formation

In the present study the structural integrity of the lipid bilayers were investigated by visual inspection of both top and cross view snapshots of bilayer systems (at different concentrations of DMSO) after a simulation time of 100 ns (Figure 5-2). As indicated in Figures 5-2 (A and B), even after a simulation time of 100 ns there was no evidence of stable pore formation in the bilayers immersed in lower concentrations of DMSO-water solutions (3 mol%

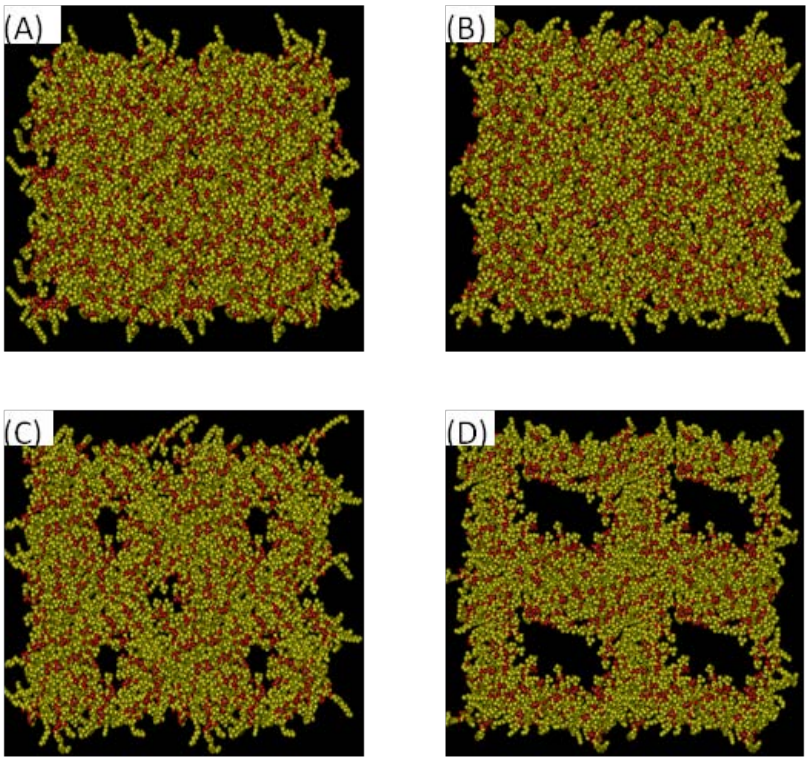

Figure 5-2: Four snapshots of DMPC bilayers after 100 ns in DMSO-water solutions at concentrations: (a) 3 mol%, (b) 6 mol%, (c) 9 mol% and (d) 11.3 mol%. For clarity, water and DMSO molecules are not shown in these top views.

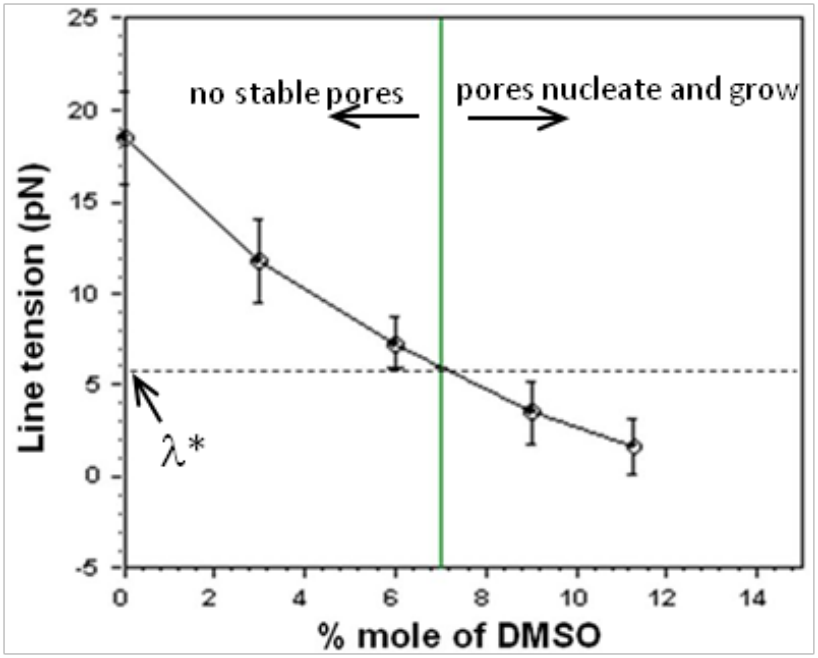

Figure 5-3: Variation of DMPC lipid bilayer line tension,λ, with the mol% of DMSO in solution.

and 6 mol%). However at higher DMSO concentrations pores are nucleated spontaneously and grow in the lipid bilayers (Figures 5-2 (C and D)). As suggested by Moldovan et al [27] the nucleation process starts with a small hydrophobic pore that grows and transforms rapidly into a hydrophilic pore.

The spontaneous nucleation of the hydrophobic pores in the 9 mol% and 11.3 mol% DMSO systems occurs after a simulation time of 23 ns and 12 ns respectively. In both systems the nucleated hydrophobic pores transform into stable hydrophilic pores that continue to grow at different rates proportional to the DMSO concentration in solution.

Table 5-1: Variation of Line tension with DMSO concentrations

mol % of DMSO	Original line tension	Line tension when 11.3 mol% DMSO is reduced to lower percentages
0	18.3 +/- 1.23	
3	11.72 +/- 1.34	6.86 +/- 1.91
6	7.26 +/- 1.26	3.43 +/- 1.34
9	3.63 +/- 1.08	2.47 +/- 1.41
11.3	1.82 +/- 1.13	1.82 +/- 1.13

From Table 5.1 it can been seen that line tension values for 3 mol% and 6 mol% DMSO system are well above the critical line tension and are in energy dominated stability region, whereas the line tension of 9 mol% DMSO and 11.3 mol% DMSO systems are below the critical line tension and are in region where pores are entropically favored. Figure 5-3 shows the MD simulation results, of the ribbon geometry bilayer systems, illustrating the variation of the actual

DMPC bilayer line tension, λ, with the concentration of DMSO in solution. As documented in Figure 5-2 and Figure 5-3 in the presence of DMSO pores nucleate spontaneously and grow in DMPC lipid bilayers only if the DMSO concentration exceeds a critical value $C_{cr} \approx 7$ mol%. Thus, the additional simulation results further lend credence to the model of pore formation proposed by Moldovan et al. [27].

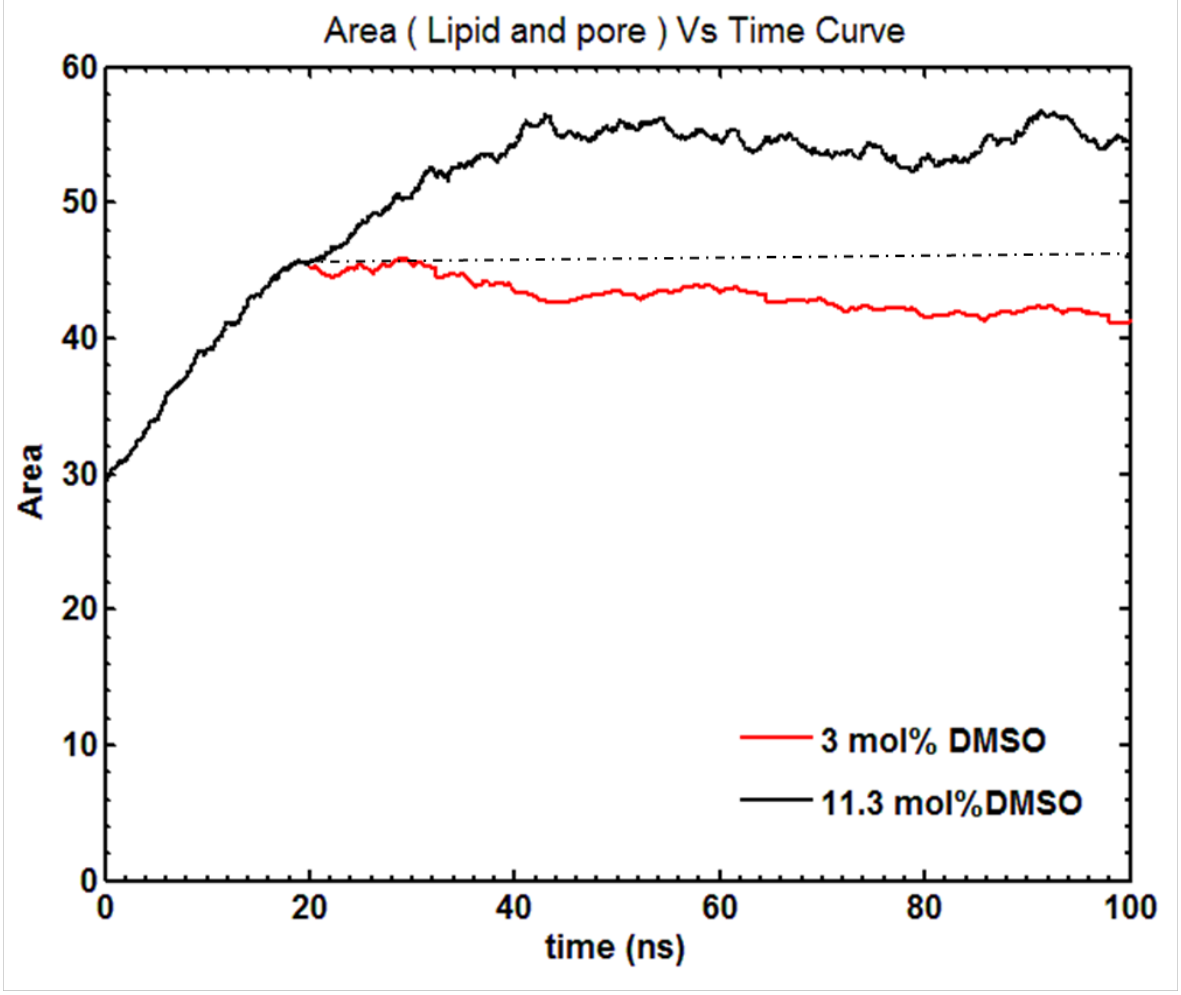

Figure 5-4: Time dependence of area of the system, 11.3 mol% DMSO system is represented in black, whereas red line denotes the system in which the concentration of DMSO had been reduced from 11.3 mol% to 3 mol% by addition of water.

It had been shown that pores can be opened and closed in lipid membranes when low voltages are applied and has been practically applied in genetic engineering to introduce macromolecules into cells and it had been used to cause cell fusion [131]. Further simulations

were performed to check if the pore nucleated at higher concentrations of DMSO [27, 47] can be closed. The simulation model chosen to check pore closure had been discussed in earlier section 5.2.

Figure 5-4 shows the change in area of the system with respect to time. For reference the area of the system of the 11.3 mol% DMSO system is also shown. From this figure it is evident that the area of the system for the case of 11.3 mol% DMSO continuously increased till 40 ns and thereafter remains constant due to the finite size of the simulated system [27] , whereas the area of the system for a reduced concentration of 3 mol% DMSO decreased by 9% and thereafter remained constant. The decrease in area of the system might be due to the decrease in area of the pore. To further investigate our pore closure results based on the critical line tension value predicted by Moldovan et al we performed few additional line tension simulations by reducing the concentration of 11.3 mol% DMSO to 3 mol%, 6 mol% and 9 mol%. The line tension values obtained for the aforementioned line tension simulations had been tabulated in Table 5.1. From the reported values shown in Table 5.1 it can be witnessed that the line tension for a pure 3 mol% DMSO simulation doesn't compare well with the case when the concentration of 11.3 mol% DMSO system is reduced to 3 mol% by addition of water, Similar results can be witnessed for 6 mol% and 9 mol% concentrations of DMSO. This result might be attributed to the fact that the addition of water molecules doesn't reduce the number of DMSO molecules accumulated near the head group regions at higher concentration of DMSO (11.3 mol%).

5.4 Conclusions and Future Work

To summarize, our MD simulations have shown that DMSO molecules perturb lipid cohesion around the pore edge in DMPC lipid bilayers leading to lowering of the line tension and the corresponding barrier for pore creation. In addition, our simulation results corroborate with

and provide atomistic support and understanding for the phenomenological theory and lattice model predictions of entropy driven pore growth studies of Shillcock and Seifert [132] and Moldovan et al [27]. On a broader scale our findings suggest that by using certain chemicals one can find ways of bringing biological membranes from the energy dominated stability regions into states in which pores are entropically favored.

The simulation performed to check the possibility of pore closure by reducing the concentration of 11.3 mol% DMSO to 3 mol% DMSO suggested that although there is no pore closure happening, there is a significant decrease in pore area. Future simulations focusing on furthermore decrease in the concentration of DMSO might yield pore closure.

REFERENCES

1. Mazur, P., *Freezing of living systems: mechanism and implications.* American Journal of Cell Physiology, 1984. **247**(3): p. C125-C142.

2. McGrath, J.J., E.G. Carvalho, and C.E. Huggins, *An experimental comparison of intracellular ice formation and freeze-thaw survival of HeLa S-3 cells.* Cryobiology, 1975. **12**(540-550).

3. Polge, C., A.U.Smith, and A.S. Parkes, *Revival of spermatozoa after vitrification and dehydration at low temperature.* Nature, 1949. **164**: p. 666-667.

4. Chi, H.J., et al., *Cryopreservation of human embryos using ethylene glycol in controlled slow freezing.* Human Reproduction, 2002. **17**: p. 2146-2151.

5. He, Y., et al., *Variation in the Membrane Transport Properties and Predicted Optimal Rates of Freezing for Spermatozoa of Diploid and Tetraploid Pacific Oyster, Crassostrea gigas.* Reprocudt. Biol., 2004. **70**: p. 1428-1437.

6. Kundu, C.N., et al., *Effect of dextrans on cryopreservation of goat cauda epididymal spermatozoa using a chemically defined medium.* Reprocduction, 2002. **123**: p. 907-913.

7. Tulandi, T. and R.G. Gosden, *Preservation of fertility*. 2004, London: Taylor & Francis Group.

8. McGrath, J.J., *Preservation of biological materials by freezing and thawing*. Heat Transfer in medicine and biology. 1985, New York: Plenum Press.

9. Palta, J.P. and P.H. Li, *Alterations in membrane transport properties by freezing injury in herbaceous plants: Evidence against rupture theory.* Plant Physiol. and Biochem., 1980. **50**: p. 169-175.

10. Fick, A., *On liquid diffusion.* Philos. Mag. J. Sci., 1855. **10**: p. 31-39.

11. Devireddy, R.V., *Predicted Permeability Parameters of Human Ovarian Tissue Cells to Various Cryoprotectants and Water*. Mol. Reprod. Dev., 2005. **70**: p. 333-343.

12. R.L.Levin, *Osmotic effects of introducing and removing permeable cryoprotectants: perfused tissues and organs.* ASME Press, 1981: p. 131-134.

13. Kedem, O. and A. Katchalsky, *Thermodynamics analysis of the permeability of biological membranes to non-electrolytes.* Biochem Biophys Acta, 1958. **27**: p. 229-246.

14. M.H.Friedman, *Principles and Models of Biological Transport*. 1986: springer-Verlag Berlin Heidelberg New York Tokyo.

15. Kimball, J.W. *Cell Membranes*. Biological Pages 2002.

16. Yeagle, P.L., *Lipid regulationof cell membrane structure and function.* FASEB J., 1989. **3**: p. 1833-1842.

17. Singer, S.J. and G.L. Nicholson, *The fluid mosaic model of the structure of cell membranes.* Science, 1972. **175**: p. 720-731.

18. Weissmann, G. and R. Claiborne, *Biochemistry, Cell Biology and Pathology*. 1975, Newyork: HP Publishing Co.

19. Fahy, E., S. Subramaniam, and H.A. Brown, *A comprehensive classification system for lipids.* Journal of Lipid Research, 2005. **46**(5): p. 839-861.

20. Langmuir, I., *The constitution and fundamental properties of solids and liquids.* J. Am. Chem. Soc., 1917. **39**: p. 1848-1906.

21. Gorter, E. and F. Grendel, *On bimolecular layers of lipoids on the chromocytes of the blood.* J. Exp. Med., 1925. **41**: p. 439-443.

22. Stein, W.D. 1985, Orlando: Academic Press

23. Fulton, T.B., *Diffusion and transport across cell membranes*. 1983, University of California: San Francisco.

24. Akhong, Q.F., et al., *Mechanisms of cell fusion.* Nature, 1975. **253**: p. 194-195.

25. Lyman, G.H., H.D.Priestler, and D. Papahadjopoulos, *Membrane action of DMSO and other chemical inducers of friend leukaemic cell differentitaion.* Nature, 1976. **262**: p. 360-363.

26. Anchordoguy, T.J., et al., *Temperature dependent perturbation od phospholipid bilayersby dimethly sulfoxide.* Biochim. Biophys. Acta., 1992. **1104**: p. 117-122.

27. Moldovan, D., D. Pinisetty, and R.V. Devireddy, *Molecular dynamics simulation of pore growth in lipid bilayer membranes in the presence of edge-active agents.* Appl. Phys. Lett., 2007. **91**: p. 204104-204107.

28. Arakawa, T., et al., *The basis for toxicity of certain cryoprotectants- a hypothesis.* Cryobiology, 1990. **27**: p. 401-405.

29. Lovelock, J.E. and M.W. Bishop, *Prevention of freezing damage to living cells by dimethly sulfoxide.* Nature, 1959. **183**: p. 1394-5.

30. Devireddy, R.V. and J.C. Bishop, *Measurement of water transport during freezing in mammalian liver tissue-part II: The use of Differential Scanning Calorimetry.* ASME J. of Biomech. Engg., 1998. **120**(559-569).

31. Kardak, A., S.P. Leibo, and R.V. Devireddy, *Freezing response of equine and macaque ovarain tissue in mixtures of dimetlysulfoxide and ethlyene glycol.* ASME J. of Biomech. Engg., 2007. **129**: p. 688-694.

32. Chang, H.H. and P.K. Dea, *Insight into the dynamics of DMSO in Phosphatidylcholine bilayers.* Biophys. Chem. , 2001. **94**: p. 33-40.

33. Tristram-Nagle, S., et al., *DMSO produces a new subgel phase in DPPC: DSC and X-ray diffraction study.* Biochim. Biophys. Acta., 1998. **1369**(1): p. 19-33.

34. Yu, Z.W. and P.J. Quinn, *Phase stability of Phosphatidylcholines in dimetlysulfoxide solutions.* biophys. j., 1995. **69**: p. 1456-1463.

35. Yu, Z.W. and P.J. Quinn, *Solvation effects of dimethylsulfoxide on the structure of phospholipid bilayers.* Biophys. Chem., 1998. **70**(1): p. 35-9.

36. Yu, Z.W. and P.J. Quinn (1998a) *The Modulation of membrane structure and stability by dimetly sulfoxide*. Mol. Membr. Biol. **15**, 59-68.

37. Gordeliy, V.I., et al., *Lipid membrane structure and interactions in dimethylsulfoxide/water mixtures.* Biophys. J., 1998. **75**: p. 2343-2351.

38. Kiselev, M.A., et al., *DMSO-induced dehydration of DPPC membranes studied by X-ray diffraction, small-angle neutron scattering, and calorimetry.* J. Alloys Comp., 1999. **86**: p. 195-202.

39. Long, C.J., et al., *The interaction of DMSO with model membranes. I. Comparison of DMSO and d6-DMSO: a DSC and IR investigation.* J. Liposome Res., 2003. **13**(3-4): p. 249-57.

40. Saiz, L. and M.L. Klein, *Electrostatic interactions in neutral model phospholipid bilayer by molecular dynamics simulations.* J. Chem. Phys., 2002. **116**: p. 3052-3057.

41. Tieleman, D.P. and H.J.C. Berendsen, *Molecular dynamics simulation of a fully hydrated dipalmitoylphosphatidylcholine bilayer with different macroscopic boundary conditions and parameters.* J. Chem. Phys. , 1996. **103**: p. 4871-4880.

42. Alper, H.E., D. Bassolino, and T.R. Stouch, *Computer simulation of a phospholipid monolayer-water system: The influence of long range forces on water structure and dynamics.* J. Chem. Phys., 1993. **98**: p. 9798-9807.

43. Bandyopadhyay, S., M. Tarek, and M.L. Klein, *Computer simulation studies of amphiphilic interfaces.* Curr. Opin. Coll. Int. Sci., 1998. **3**: p. 242-246.

44. Bemporad, D., J.W. Essex, and C. Luttmann, *Permeation of small molecules through a lipid bilayer: A computer simulation study.* J. Phys. Chem. B. , 2004. **108**: p. 4875-4884.

45. Berendsen, H.J.C. and S.-J. Marrink, *Molecular dynamics of water transport through membranes: Water from solvent to solute.* Pure and Applied Chem. , 1993. **65**: p. 2513-2520.

46. Goetz, R. and R. Lipowsky, *Computer simulation of bilayer membranes: self-assembly and interfacial tension.* J. Chem. Phys. , 1998. **108**: p. 7397-7409.

47. Gurtovenko, A.A. and J. Anwar, *Modulating the structure and properties of cell membranes: the molecular mechanism of action of dimethyl sulfoxide.* J. Phys. Chem. B, 2007. **111**(35): p. 10453-60.

48. Marrink, S.J. and H.J.C. Berendsen, *Permeation process of small molecules across lipid membranes studied by molecular dynamics simulations.* J. Phys. Chem. , 1996. **100**: p. 16729-16738.

49. Smondyrev, A.M. and M.L. Berkowitz, *Molecular dynamics simulation of DPPC bilayer in DMSO.* Biophys. J., 1999. **76**(5): p. 2472-8.

50. Sum, A.K., *Molecular simulation study of the influence of small molecules on the dynamic and structural properties of phospholipid bilayers.* Chem. Biodivers., 2005. **2**(11): p. 1503-16.

51. Sum, A.K. and J.J. de Pablo, *Molecular simulation study on the influence of dimethylsulfoxide on the structure of phospholipid bilayers.* Biophys. J., 2003. **85**(6): p. 3636-45.

52. Paci, E. and M. Marchi, *Membrane crossing by a polar molecule: A molecular dynamic simulation.* Mol. Simul., 1994. **14**: p. 1-10.

53. Pinisetty, D., D. Moldovan, and R.V. Devireddy, *The effect of methanol on lipid bilayers: An atomistic investigation.* Annals of Biomed. Engg., 2006. **34**: p. 1442-1451.

54. Alder, B.J. and T.E. Wainwright, *Phase transition for a hard sphere system.* J. Chem. Phys., 1957. **27**: p. 1208-1209.

55. Rahman, A., *Correlations in the motion of atoms in liquid argon.* Phys. Rev., 1964. **136**: p. A405-A411.

56. Stillinger, F.H. and A. Rahman, *Improved simulation of liquid water by molecular dynamics.* J. Chem. Phys. , 1974. **60**: p. 1545-1557.

57. Frenkel, D. and B. Smit, *Understanding molecular simulation*. 1996, San Diego: Academic Press.

58. Lindahl, E., B. Hess, and D.V.d. Spoel, *GROMACS 3.0: A package for molecular simulation and trajectory analysis.* J. Mol. Mod. , 2001. **7**: p. 306-317.

59. Verlet, L., *Computer "Experiments" on Classical Fluids. I. Thermodynamical Properties of Lennard-Jones Molecules.* Phys. Rev., 1967. **159**: p. 98-103.

60. Hockney, R.W. and J.W. Eastwood, *Computer simulations using particles*. 1981, London: McGraw Hill.

61. Edberg, R., D.J. Evans, and G.P. Morriss, *Constrained Molecular-Dynamics Simulations of Liquid Alkanes with a New Algorithm.* J. Am. Chem. Phys., 1986. **84**: p. 6933-6939.

62. Baranyai, A. and D.J. Evans, *New Algorithm for Constrained Molecular-Dynamics Simulation of Liquid Benzene and Naphthalene.* Mol. Phys., 1990. **70**: p. 53-63.

63. Hess, B., et al., *LINCS: A linear constraint solver for molecular simulations.* J. Comp. Chem. , 1997. **18**: p. 1463-1472.

64. Wiener, M.C. and S.H. White, *Structure of a fluid dioleoylphosphatidylcholine bilayer determined by joint refinement of x-ray and neutron diffraction data. II. Distribution and packing of terminal methyl groups.* Biophys. J., 1992. **61**: p. 428-433.

65. Hristova, K. and S.H. White, *Determination of the hydrocarbon core structure of fluid dioleoylphosphocholine (DOPC) bilayers by x-ray diffraction using specific bromination of the double-bonds: Effect of hydration.* Biophys. J., 1998. **74**: p. 2419-2433.

66. Tristram-Nagle, S., et al., *Thermodynamic and Structural Characterization of Amino-Acid Linked Dialkyl Lipids.* Chem. Phys. Lipids, 2005. **134**(29-39).

67. Tristram-Nagle, S., et al., *Measurement of Chain Tilt Angle in Fully Hydrated Bilayers of Gel Phase Lecithins.* Biophys. J., 1993. **64**: p. 1097-1109.

68. Bloom, M., E. Evans, and O. Mouritsen, *Physical properties of the fluid lipid-bilayer component of cell membranes: A perspective.* Q. Rev. Biophys. , 1991. **24**: p. 293-397.

69. Brown, M.F., A.A. Ribeiro, and G.D. Williams, *New view of lipid bilayer dynamics from 2H and 13C NMR relaxation time measurements.* Proc Natl Acad Sci U S A, 1983. **80**: p. 4325-9.

70. Ulrich, A.S. and A. Watts, *Molecular response of the lipid headgroup to bilayer hydration monitored by 2H-NMR.* Biophys. J., 1994. **66**: p. 1441-1449.

71. Volke, F., et al., *Dynamic properties of water at phosphatidylcholine lipid-bilayer surfaces as seen by deuterium and pulsed field gradient proton NMR.* Chem. Phys. Lipids, 1994. **70**: p. 121-131.

72. Mendelsohn, R. and L. Senak, *Quantitative determination of conformational disorder in biological membranes by FTIR spectroscopy*, ed. J.R. Clark and R.E. Heister. 1993, Newyork: Wiley.

73. Chang, H.H. and P.K. Dea, *Insights into the dynamics of DMSO in phosphatidylcholine bilayers.* Biophys. Chem., 2001. **94**(1-2): p. 33-40.

74. Feller, S.E., *Molecular dynamics simulations of lipid bilayers.* J. Curr Opin. Coll. Int. Sci., 2000. **5**: p. 217-223.

75. Pastor, R.W., *Molecular dynamics and Monte Carlo simulations of lipid bilayers.* Curr. Opin. Struct. Biol. , 1995. **4**: p. 486-492.

76. Weiner, S.J., et al., *A new force feild for molecular mechanical simulation of nucleic acids and proteins.* J. Am. Chem. Soc., 1984. **106**: p. 765-784.

77. Brooks, B.R., et al., *CHARMM: A Program for Macromolecular Energy, Minimization, and Dynamics Calculations.* J. Comp. Chem., 1983. **4**: p. 187-217.

78. Hermans, J., et al., *A consistent empirical potential for water-protein interactions.* Biopolymers, 1984. **23**: p. 1513-1518.

79. Jorgensen, W.L. and J.Tirado-Rives, *The OPLS potential function for proteins, Energyminimization for crystals of cyclic peptides and crambin.* J. Am. Chem. Soc., 1988. **110**: p. 1657-1666.

80. Ploeg, P.V.d. and H.J.C. Berendsen, *Molecular dynamics simulation of a bilayer membrane.* J. Chem. Phys., 1982. **76**: p. 3271-3276.

81. Ploeg, P.V.d. and H.J.C. Berendsen, *Molecular dynamics of a bilayer membrane.* Mol. Phys., 1983. **49**: p. 233-248.

82. Egberts, E., *Molecular dynamic simulations of multibilayer membranes* 1988, University of Groningen: Nertherlands.

83. Egberts, E., S.J. Marrink, and H.J.C.Berendsen, *Molecular dynamics simulation of a phospholipid membrane.* Eur. Bioph. J., 1994. **22**: p. 423-436.

84. Pastor, R.W., R.M. Venable, and M. Karplus, *Model for the structure of the lipid bilayer.* Proc. Natl. Acad. Sci., 1991. **88**: p. 892-896.

85. Berkowitz, M.L. and K. Raghavan, *Computer simulation of a water/membrane interface.* Langmuir, 1991. **7**: p. 1042-1044.

86. Biswas, A. and B.L. Schurmann, *Molecular dynamics simulation of a dense model bilayer of chain molecules with fixed head groups.* J. Chem. Phys. , 1991. **95**: p. 5377-5386.

87. Husslein, T., et al., *Constant pressure and temperature molecular-dynamics simulation of the hydrated diphytanolphosphatidylcholine lipid bilayer.* J. Chem. Phys. , 1998. **109**: p. 2826-2832.

88. Mashl, R.J., et al., *Molecular simulation of dioleoylphosphatidylcholine lipid bilayers at differing levels of hydration.* Biophys. J., 2001. **81**: p. 3005-3015.

89. Venable, R.M., B.R. Brooks, and R.W. Pastor, *Molecular dynamics simulations of gel phase lipid bilayers in constant pressure and constant surface area ensembles.* J. Chem. Phys., 2000. **112**: p. 4822-4832.

90. Essman, U. and M.L. Berkowitz, *Dynamical properties of phospholipid bilayers from computer simulation.* Biophys. J., 1999. **76**: p. 2081-2089.

91. Lindahl, E. and O. Edholm, *Mesoscopic undulations and thickness fluctuations in lipid bilayers from molecular dynamics simulations.* Biophys. J., 2000. **79**: p. 426-433.

92. Bandyopadhyay, S., M. Tarek, and M.L. Klein, *Molecular dynamics study of a lipid-DNA complex.* J. Phys. Chem. B 1999. **103**: p. 10075-10080.

93. Berger, O., O. Edholm, and F. Jahnig, *Molecular dynamics simulations of a fluid bilayer of dipalmitoylphosphatidylcholine at full hydration, constant pressure, and constant temperature.* Biophys. J., 1997. **72**: p. 2002-2013.

94. Duong, T.H., E.L. Mehler, and H. Weinstein, *Molecular dynamics simulation of membranes and a transmembrane helix.* J. Comp. Phys., 1999. **151**: p. 358-387.

95. Haile, J.M., *Molecular Dynamics Simulation: Elementary Methods*. 1992, New York: Wiley.

96. Leekumjorn, S. and A.K. Sum, *Molecular study of the diffusional process of DMSO in double lipid bilayers.* Biochim. Biophys. Acta., 2006. **1758**(11): p. 1751-8.

97. Marrink, J., D.P. Tieleman, and A.E. Mark, *Molecular dynamics simulations of the kinetics of spontaneous micelle formation.* J. Phys. Chem. B, 2000. **104**: p. 12165-12173.

98. Marrink, S.J. and H.J.C. Berendsen, *Simulation of water transport through a lipid-membrane.* J. Phys. Chem., 1994. **98**: p. 4155-4168.

99. Marrink, S.J., et al., *Simulation of the spontaneous aggregation of phospholipids into bilayers.* J. Am. Chem. Soc., 2001. **123**: p. 8638-8639.

100. Notman, R., et al., *The permeability enhancing mechanism of DMSO in ceramide bilayers simulated by molecular dynamics.* Biophys. J., 2007. **93**(6): p. 2056-68.

101. Notman, R., et al., *Molecular basis for dimethylsulfoxide (DMSO) action on lipid membranes.* J. Am. Chem. Soc., 2006. **128**(43): p. 13982-3.

102. Essman, U., L. Perera, and M.L. Berkowitz, *The origin of the hydration interaction of lipid bilayers from MD simulation of dipalmitoylphosphatidylcholine membranes in gel and liquid crystalline phases.* Langmuir, 1995. **11**: p. 4519-4531.

103. Söderhäll, J.A. and A. Laaksonen, *Molecular dynamics simulation of ubiquinone inside a lipid bilayer.* J. Phys. Chem. B 2001. **105**: p. 9308-9315.

104. Smondyrev, A.M. and M.L. Berkowtiz, *Structure of DPPC/cholestrol bilayer at low and high cholestrol concentrations:molecular dynamic simulation.* biophys. J., 2001. **77**: p. 2075-2089.

105. Tu, K., M.L. Klein, and D.J. Tobias, *Constant-pressure molecular dynamics investigation investigation of cholestrol effects in a DPPC bilayer.* Biophys. J., 1998. **75**: p. 2147-2156.

106. López-Cascales, J.J. and J.G.d.l. Torre, *Effect of lithium and sodium ions on a charged membrane of dipalmitoylphosphatidylserine: a study by molecular dynamic simulations.* Biochem Biophys Acta, 1997. **1330**: p. 145-156.

107. Casares, J.J.G., et al., *Effect of Na+ and Ca2+ ions on a lipid langmuir monolayer: an atomistic description by molecular dynamic simulations.* Chem. Phys. , 2008. **9**: p. 2538-2543.

108. Lindahl, E. and M.S. Sansom, *Membrane proteins: molecular dynamic simulations.* Curr. Opin. Struct. Biol., 2008. **18**: p. 425-431.

109. Meyer, F.J.d., M. Vistoli, and B. Smit, *Molecular simulations of lipid-mediated protein-protein interactions.* Biophys. J., 2008. **95**: p. 1851-1865.

110. Bassolino-Klimas, D., H.E. Alper, and T.R. Stouch, *Solute diffusion in lipid bilayer membranes: An atomistic level study by molecular dynamic simulation.* Biochemistry, 1993. **32**: p. 12624-37.

111. Bassolino-Klimas, D., H.E. Alper, and T.R. Stouch, *Mechanism of solute diffusion through lipid bilayer-membranes by molecular dynamics simulation.* J. Am. Chem. Soc. , 1995. **117**: p. 4118-4129.

112. Berendsen, H.J.C., et al., *Molecular dynamics with coupling to an external bath.* J. Chem. Phys., 1984. **81**: p. 3684-3690.

113. Berendsen, H.J.C., et al., *Interaction models for water in relation to protein hydration, in `Intermolecular Forces'*, ed. B. Pullman and Reidel. 1981, Dordrecht.

114. Marrink, S.J., R.M. Sok, and H.J.C. Berendsen, *Free volume properties of a simulated lipid membrane.* J. Chem. Phys. , 1996. **104**: p. 9090-9099.

115. Yamashita, Y., K. Kinoshita, and M. Yamazaki, *Low concentration of DMSO stabilizes the bilayer gel phase rather than the interdigitated gel phase in dihexadecylphosphatidylcholine membrane.* Biochim. Biophys. Acta., 2000. **1467**(2): p. 395-405.

116. Essman, U., et al., *A smooth particle mesh Ewald method.* J. Chem. Phys., 1995. **103**: p. 8577-8593.

117. Pandit, S.A., D. Bostick, and M.L. Berkowitz, *An algorithm to describe molecular scale rugged surfaces and its application to the study of a water/lipid bilayer interface.* J. Chem. Phys., 2003: p. 2199-2205.

118. Anchordoguy, T.J., et al., *Temperature-dependent perturbation of phospholipid bilayers by dimethylsulfoxide.* Biochim. Biophys. Acta., 1992. **1104**(1): p. 117-22.

119. Landau, L.D. and E.M. Lifshitz, *Statistical Physics*. 1980, Louis: Pergamon Press

120. Liu, H., F. Muller-Plathe, and W.F.V. Gunsteren, *A force field for liquid dimethylsulfoxide and physical properties of liquid dimethylsulfoxide calculated using molecular dynamics simulation.* J. Am. Chem. Soc. , 1995. **117**: p. 4363-4366.

121. Luzar, A. and D. Chandler, *Structure and hydrogen-bond dynamics of water-dimethylsulfoxide mixtures by computer-simulations.* J. Chem. Phys. , 1993. **98**: p. 8160-8173.

122. Rao, B.G. and U.C. Singh, *A free-energy perturbation study of solvation in methanol and dimethylsulfoxide.* J. Am. Chem. Soc., 1990. **112**: p. 3803-3811.

123. Vaisman, I.I. and M.L. Berkowitz, *Local structural order and molecular associations in water-DMSO mixtures: Molecular dynamics study.* J. Am. Chem. Soc. , 1992. **114**: p. 7889-7896.

124. Gurtovenko, A.A., *Asymmetry of lipid bilayers induced by monovalent salt: Atomistic molecular-dynamic study.* J. Chem. Phys., 2005. **122**: p. 244902.

125. Bostick, D. and L. Berkowitz, *The implementation of slab geomentry for membrane-channel molecular dynamics simulations.* Biophys. J., 2003. **85**: p. 97-107.

126. Lee, S.J., Y. Song, and N.A. Baker, *Molecular dynamics simulations of Asymmetric NaCl and KCl solutions seperated by Phosphatidylcholine Bilayers: Potential drops and structural changes induced by strong Na+ - lipid interactions and finite size effects.* Biophys. J., 2008. **94**: p. 3565-3576.

127. Leontiadou, H., A.E. Mark, and S.J. Marrink, *Molecular dynamic Simulations of Hydrophilic Pore in Lipid Bilayers.* Biophys. J., 2004. **86**: p. 2156-2164.

128. Tieleman, D.P., et al., *Simulation of Pore Formation in Lipid Bilayers by Mechanical Stress and Electric Fields.* J. Am. Chem. Soc., 2003. **125**: p. 6382-6383.

129. Tolpekina, T.V., W.K. denOtter, and W.J. Briels, *Simulations of stable pores in membranes: System size dependence and line tension.* J. Chem. Phys, 2004. **121**: p. 1442-1451.

130. Lister, J.D., *Stability of lipid bilayers and red blood cell membranes.* Phys. Lett., 1975. **53A**: p. 193-194.

131. Kalinowski, S. and Z. Figaszewski, *A four-electrode potentiostat-galvanostat for studies of bilayer lipid membranes.* Meas. Sci. Technol., 1995. **6**: p. 1050-1055.

132. Shillcock, J.C. and U. Seifert, *Thermally Induced Proliferation of Pores in a Model Fluid Membrane.* Biophys. J., 1998. **74**: p. 1754-1766.

VITA

Raghava Alapati was born in December, 1984, in Edlapalli, Andrapradesh, India. He received his Bachelor of Technology in mechanical engineering from Jawaharlal Nehru Technological University, Hyderabad, Andrapradesh, India, in May 2006. He enrolled in the Department of Mechanical Engineering at Louisiana State University, Baton Rouge, Louisiana, in August 2006 to attend graduate school. He is a candidate for the degree of Master of Science in Mechanical Engineering to be awarded at the commencement of December, 2009.